

Learned iterative networks: An operator learning perspective

Andreas Hauptmann* Ozan Öktem†

December 10, 2025

Abstract

Learned image reconstruction has become a pillar in computational imaging and inverse problems. Among the most successful approaches are learned iterative networks, which are formulated by unrolling classical iterative optimisation algorithms for solving variational problems. While the underlying algorithm is usually formulated in the functional analytic setting, learned approaches are often viewed as purely discrete. In this chapter we present a unified operator view for learned iterative networks. Specifically, we formulate a learned reconstruction operator, defining *how to compute*, and separately the learning problem, which defines *what to compute*. In this setting we present common approaches and show that many approaches are closely related in their core. We review linear as well as nonlinear inverse problems in this framework and present a short numerical study to conclude.

Keywords: Inverse problems, machine learning, operator learning, algorithm unrolling, learned iterative schemes.

1 Introduction

Data-driven approaches, and in particular machine learning approaches based on deep neural networks (deep learning) [96], have shown unparalleled capability in performing a variety of tasks. Initial success stories related to tasks in natural language processing [8, 25, 151] and computer vision [80, 87, 145], but recent success relates to performing more complex tasks [97, 149, 155]. This has in turn catalysed a surge of interest in applying such data driven learning techniques for performing a variety of computing tasks in science and engineering, like solving ill-posed inverse problems.

As will be outlined in this chapter, usage of deep learning in such applications often requires invoking *structured learning*. This refers loosely to various techniques for domain adaptation that go beyond choosing domain specific training data and loss function. Here, we focus particularly on *learned iterative networks*, which represent a specific form of structured learning that is suited for learning

*Research Unit of Mathematical Sciences, University of Oulu, Finland and Department of Computer Science, University College London, United Kingdom.

†Department of Mathematics, KTH - Royal Institute of Technology, Sweden

tasks that are given as iterative schemes. The idea is to parametrise the learning by means of such an iterative scheme. As such, learned iterative networks can be useful for learning any task that is representable as an iterative scheme, like finding a minimiser or solving an ill-posed inverse problem.

Overview The overarching viewpoint of this chapter is built around an operator learning perspective for solving inverse problems. The inverse problem is given by an operator equation and solving it with a (learned) reconstruction method corresponds to defining and training a *learned reconstruction operator*.

Defining the learning within such a functional analytic viewpoint yields a unified and structured description of various machine-learning methods for solving inverse problems. For learned iterative networks, this includes in particular many popular architectures, like learned gradient schemes [6], learned proximal networks [59], and variational networks [66, 92]. We will also notice that there is a significant conceptual overlap between these architectures when they are viewed as an operator learning problem. Additionally, the above approach also allows us to decouple the formulation of the learned reconstruction operator from the learning task, where the latter is more concerned about how to train the learned reconstruction operator.

Thus, this chapter will first formulate the operator learning problem in Section 2 and its application to inverse problems with the definition of a *learned reconstruction operator*. We continue to discuss the concept of *structured learning* in Section 3, enabling learning the reconstruction operator by domain adaptation to the inverse problem at hand. Section 4 introduces the *learning problem*, i.e., the question of training data and loss functions. With these preliminaries we move to *neural operator architectures* in Section 5, where *learned iterative networks* are introduced along with a short historical account. Section 6 concentrates on learned iterative methods based on gradient based optimisation methods, whereas 7 discusses primal-dual architectures. We will then discuss non-linear inverse problems and higher order methods such as Newton type approaches in Section 8. The chapter concludes with two Section concentrating on the practical side with implementation related aspects in Section 9 and numerical examples providing a performance comparison 10.

2 Operator learning

Many computing tasks in science and engineering can be formulated as approximating a mapping whose domain and range is allowed to be infinite dimensional Hilbert or Banach spaces. This functional analytic setting is commonly used when characterising mathematical properties of the aforementioned approximation in a way that is independent of the choice of discretisation. It is then natural to consider (deep) learning in the same functional analytic setting, which brings us to *operator learning*.

Stated more formally, operator learning aims to use data-driven techniques from machine learning to discover or approximate a mapping, the *target operator*,

$$\mathcal{R}: Y \rightarrow X. \tag{1}$$

Here, X and Y are possibly infinite dimensional spaces that are endowed with probability measures. We will work in the setting where X and Y are Hilbert

spaces. The *architecture* of the neural operator is a precise parametrisation of the family of operators used for the approximation, i.e., a specification of a family $\{\mathcal{R}_\theta\}_{\theta \in \Theta}$ where $\mathcal{R}_\theta: Y \rightarrow X$ with a parameter set Θ that is a finite dimensional vector space.

An important part of operator learning is to extend common neural network architectures, which parametrise mappings between finite dimensional spaces, to the above functional analytic setting where the domain and range can be infinite dimensional spaces (*neural operators*). The choice of architecture strongly influences approximation and stability properties of the learned neural operator. This is particularly important in solving inverse problems [17, 70, 113].

2.1 Inverse problem solvers (learned reconstruction)

Consider the inverse problem of finding the *signal* $f \in X$ from *data* $g \in Y$ that is given as

$$g = \mathcal{A}(f) + e. \quad (2)$$

Here, $e \in Y$ represents the (unknown) observation error and (possibly non-linear) forward operator $\mathcal{A}: X \rightarrow Y$ is a known mapping that models how observed data in Y is generated by a signal in X in absence of noise. In many cases, like computed tomography (CT), it is possible to pre-process data so that the corresponding forward operator is linear. Other inverse problems, like electrical impedance tomography (EIT), are intrinsically non-linear in the sense that it is not possible to pre-process data or transform the problem without simplifications so that it becomes linear.

A solution method for the inverse problem in (2) is represented by a *reconstruction operator* $\mathcal{R}: Y \rightarrow X$ that approximates some form of (pseudo) inverse of the forward operator. The reconstruction operator should ideally be stable and provide a good approximation to the original hidden signal f that gives rise to observed data g , i.e., $\mathcal{R}(g) \approx f$ whenever $g \approx \mathcal{A}(f)$. Classically, such a reconstruction operator is handcrafted based on the knowledge about the forward operator and its inverse, or formulated in the variational framework as an optimisation problem. However, it is also possible to learn a reconstruction operator from example data. The formal definition is given as follows.

Definition 2.1 (Learned reconstruction operator). A family of parametrised mappings

$$\mathcal{R}_\theta: Y \rightarrow X \quad \text{where } \theta \in \Theta$$

along with a specification of the parameter set Θ is called a *learned reconstruction operator* for the inverse problem in (2) if the parameters θ are determined (learned) from example data (training data) that is generated in a way that is consistent with (2).

The above definition does not touch upon how to choose the architecture for the learned reconstruction operator, i.e., how it is parametrised. This is important and *learned iterative networks*, which constitute the central theme for the entire chapter, deal with this question when the target operator is given by an iterative scheme.

2.2 Optimisation solvers (learning-to-optimise)

Operator learning can also be used for performing other computing tasks, like accelerating an optimisation solver. The aim is then to train a neural operator so that it approximates a target operator $\mathcal{R}: Y \rightarrow X$ that minimises a convex objective. The objective belongs to a class of functionals $\mathcal{E}_g: X \rightarrow \mathbb{R}$ that is parametrised by $g \in Y$, so the target operator is expressible as

$$\mathcal{R}(g) := \arg \min_{f \in X} \mathcal{E}_g(f) \quad \text{for } g \in Y. \quad (3)$$

One now needs to set-up the appropriate learning problem so that training the neural operator $\mathcal{R}_\theta: Y \rightarrow X$ corresponds to approximating \mathcal{R} (learning-to-optimise). One way to set-up the learning problem would be to use the objective function as the loss as in [26, 27]. This is similar to approaches for solving a partial differential equation (PDE) based on physics-informed neural networks (PINNs) where the loss-function consists of the PDE and its boundary conditions. Other similar approaches are nicely surveyed in [39, Section 4]. We will discuss a possible training shortly in Section 4.2.

It is important to note that learned iterative networks that are based on an optimisation solver do not automatically fall under learning-to-optimise, if the corresponding learning problem is not appropriately chosen. In particular, the majority of unrolling methods that will be discussed later are different to learning-to-optimise.

3 Structured learning

Operator learning can quickly become challenging due to difficulties in ensuring sufficient generalisation and handling scalability issues. This applies to both solving ill-posed inverse problems as well as solving optimisation problems.

Inverse problems are often ill-posed meaning that solution methods that only seek to fit observed data will amplify observation errors. Additionally, despite clever discretisations, many inverse problems lead to large-scale numerical computations since elements in the domain and range of the forward operator need to be represented with very high-dimensional arrays. Likewise, solving optimisation problems that arise in high dimensional signal and image processing quickly lead to large-scale numerical computations. This is especially the case in imaging applications. Adopting a naive ‘discretise first, then train’ approach means using a trained neural network for solving very large-scale ill-posed inverse problems. Doing this with reasonable accuracy and generalisation properties is challenging. In particular, using generic neural network architectures and then relying entirely on the scaling law is not a feasible approach as we briefly argue for in Section 5.2.

The solution to the above scaling challenge is to use *structured learning*. This refers to domain adaptation that goes beyond choosing appropriate training data. The key component in structured learning is to incorporate additional (handcrafted) ‘structure’ into the data-driven approach for performing the task.

The subsequent sections list some common forms of structure that is used in constructing a domain adapted architecture for the neural operator. Such techniques for structured learning are gaining momentum in applications of deep learning to various computing related tasks in science and engineering. A key

factor is the emergence of techniques for incorporating different type of structure into the neural operator architecture or the loss function used in training. Such structure is essential for using neural operators to solve high-dimensional ill-posed inverse problems, where domain adaptation is necessary for designing robust inverse modelling techniques. Data-driven methods based on structured learning have had considerable success in matching, or outperforming, state-of-the-art while at the same time offering a significant computational speed-up. On a final note, the majority of structured data-driven approaches still come without formal mathematical guarantees, such as sample complexity results, accuracy guarantees, or useful estimates of the generalisation gap. While we cannot address this shortcoming, Section 5.3 aims to provide a survey of learned iterative networks, which are a type of physics informed architectures that have been very successful in solving inverse problems.

3.1 Group symmetries and equivariances

Many tasks are represented by a target operator \mathcal{R} in (1) that has group symmetries or equivariances. State mathematically, G -equivariance with respect to a group G that acts on Y and X means

$$\mathcal{R} \circ T_Y(\phi) = T_X(\phi) \circ \mathcal{R} \quad \text{for any } \phi \in G,$$

where $T_Y(\phi): Y \rightarrow Y$ and $T_X(\phi): X \rightarrow X$ denote the (group) actions of ϕ on Y and X , respectively. It is then natural to require that the neural operator \mathcal{R}_θ approximating \mathcal{R} also has the same group equivariance. In fact, the very popular convolutional neural networks (CNNs) are a translation equivariant architecture used for many imaging tasks.

3.2 Simulator informed architectures

In many tasks, there is often (partial) knowledge about how data associated with the task is generated. One can then seek neural operator architectures for approximating the target operator \mathcal{R} in (1) that accounts for such a simulator, e.g., by incorporating explicit operator(s) associated with simulating and modelling data (simulator informed architectures). As an example, when solving inverse problems it is natural to account for the forward operator (simulator) and its adjoint (for linear forward operators) or adjoint of its Fréchet derivative (for non-linear forward operators).

A common example of the above is when one has an initial approximation $\mathcal{R}_0: Y \rightarrow X$ of \mathcal{R} in (1) that implicitly accounts for how data is generated. This can be used to define a learned reconstruction operator as *pre/post-processing architectures*, which are neural operator architectures of the form

$$\mathcal{R}_\theta := \Lambda_{\theta_{\text{post}}}^{\text{post}} \circ \mathcal{R}_0 \circ \Lambda_{\theta_{\text{pre}}}^{\text{pre}} \quad \text{with } \theta = (\theta_{\text{pre}}, \theta_{\text{post}})$$

where $\Lambda_{\theta_{\text{pre}}}^{\text{pre}}: Y \rightarrow Y$ and $\Lambda_{\theta_{\text{post}}}^{\text{post}}: X \rightarrow X$ represent learned pre- and post-processing operators. The most common choice are networks that represent some form of learned restoration and denoising networks, which can be trained separately. Post-processing networks would be trained to improve the output from \mathcal{R}_0 [82, 85]. For pre-processing networks these would remove measurement

noise or fill missing parts of data. Finally, a joint training of both is possible, which is sometimes also referred to as dual-domain approach [101].

Pre/post-processing architectures are popular due to their simplicity and success, especially in solving mildly ill-posed inverse problems arising in imaging. *Learned iterative networks* represent a further refinement of these. The idea is to have a neural operator $\mathcal{R}_\theta: Y \rightarrow X$ with an architecture that is derived from an iterative scheme which defines the target operator $\mathcal{R}: Y \rightarrow X$ one seeks to approximate. Hence, we assume there is an iterative scheme $(f^k)_k \subset X$ (depending on $g \in Y$) such that $\mathcal{R}(g) = \lim_{k \rightarrow \infty} f^k$. The neural operator $\mathcal{R}_\theta: Y \rightarrow X$ is then given by first truncating this iterative scheme, then replacing handcrafted updates with neural operators (unrolling). This can be done in different ways, thus resulting in different neural operator architectures as outlined in Section 5.3.

3.3 Multi-scale architectures

Many tasks involve data that comes from multi-scale phenomena. The target operator \mathcal{R} in (1) representing the task will then have specific structure that can be used in approximating it. An example is when \mathcal{R} admits a hierarchical multi-scale decomposition that numerical methods often utilise, e.g., with H - or H^2 -matrices and tensors. This is indeed the case when \mathcal{R} is a pseudodifferential operator, as is the case when it represents the inverse of the ray transform.

It is now natural to account for such multi-scale structure in the design of the deep neural operator architecture (multi-scale architectures). One can in particular leverage on operator decomposition and compression techniques developed within multi-scale numerical methods. Based on this, one can consider various neural network architectures that are designed around such a hierarchical operator decomposition. These have been used for approximating pseudodifferential or Fourier integral operators as shown in [53, 54, 55, 56, 98], see also [57] for a similar approach for inverting the ray transform.

Remark 3.1. *It is also worth mentioning domain adaptations that manifest themselves in terms of specific choices of network components, like using convolution, attention, encoder/decoder with skip connections (think U-Net and U-former), scale space models, architectures based on Fourier Neural Operators (FNOs), etc., see discussion in Section 5.1.*

4 Learning problems

The concept of a learned reconstruction operator $\mathcal{R}_\theta: Y \rightarrow X$ for the inverse problem in (2) was introduced in Section 2.1. While this operator provides the architectural basis for the mapping between data space Y and image space X , the parameters θ can be obtained in various ways. This depends on the type of training data available and possible cost functions that can be formulated for the training procedure.

The above two components influence how to set up the training procedure for the operator learning, which we henceforth refer to as the *learning problem*. In fact, as we will show, the same reconstruction operator can be trained in different ways depending on the chosen learning problem. These choices are correspond to usage of different concepts from machine learning in solving inverse problems.

To prepare for discussing the various different ways of setting up the learning problem, we distinguish between two primary cases for training data in inverse problems: fully *supervised* and *unsupervised* data.

The first setting, the supervised case, assumes access to example data (training data) of the form

$$(f_1, g_1), \dots, (f_n, g_n) \in X \times Y$$

that are independent identically distributed (IID) random draws from an $(X \times Y)$ -valued random variable (f, g) that satisfies the operator equation (2). While this is the desired case from a learning perspective, it is not the usual case for inverse problems to have access to a large set of ground-truth samples.

The second case, the unsupervised setting, is therefore the most natural one for inverse problems. Here we only have training data that consists of the observed data, i.e., samples $g_1, \dots, g_n \in Y$ that are generated by a Y -valued random variable g . Alternatively, we also consider the case where samples $f_1, \dots, f_n \in X$ by a X -valued random variable f are given.

4.1 Supervised operator learning

The most common setting for supervised learning is with a loss function in X , i.e., $\mathcal{L}_X: X \times X \rightarrow \mathbb{R}$, like a p -norm. The learned reconstruction operator \mathcal{R}_θ can then be defined as the associated Bayes estimator, which is given as $\mathcal{R}_{\hat{\theta}}: Y \rightarrow X$ where $\hat{\theta} \in \Theta$ solves the following learning problem:

$$\hat{\theta} \in \arg \min_{\theta \in \Theta} \mathbb{E}_{(f, g)} \left[\mathcal{L}_X(\mathcal{R}_\theta(g), f) \right]. \quad (4)$$

In practice we only have finite number of samples $(f_1, g_1), \dots, (f_n, g_n) \in X \times Y$ from (f, g) . Hence, instead of solving the learning problem in (4), we compute the corresponding empirical risk estimator by solving the training problem

$$\hat{\theta} \in \arg \min_{\theta \in \Theta} \sum_{i=1}^n \mathcal{L}_X(\mathcal{R}_\theta(g_i), f_i). \quad (5)$$

Supervised learning is the most often considered setting in the literature, since it is in fact the most desirable case for learned reconstruction. This is simply because the learning involves training data that provide access to ground-truth/measurement pairs which are directly linked by the underlying operator equation and hence carry the most information of the inverse problem. But, this is also its main drawback, namely that each observed data in the training data needs to have a corresponding ground-truth signal. This can be problematic to obtain in practice.

4.2 Unsupervised operator learning

It is often difficult to gain access to paired training examples that are drawn from the joint distribution of the $(X \times Y)$ -valued random variable (f, g) .

To illustrate the difficulty, consider setting up the learning problem of learned reconstructions for low-dose CT image reconstruction. Supervised data would in this context consist of pairs $(f_i, g_i) \in X \times Y$ where f_i is the true image and

g_i is the low-dose CT data generated by f_i (see Section 4.1). Experimentally acquiring such data is challenging since it is difficult to get access to the true image f_i that generated the low-dose data g_i . A typical approach would be to scan the object twice, one high-dose scan and one low-dose scan. The former is used for computing the ‘true’ image f_i . One also needs to align the ‘true’ image to the image reconstructed from corresponding low-dose data to ensure exact correspondence (one could avoid this step by using a loss that is invariant to rigid body transformations, see e.g. [7]). Supervised training in CT image reconstruction is for these reasons commonly based on simulated data.

Consequently, a more practical setting in inverse problems is when training data represent IID samples from the marginal distribution of f or g . More precisely, one typically encounters one of the following three scenarios (or, some combinations thereof) that we now outline.

Remark 4.1. *We only present a subset of possible learning problems to provide an intuition on potential formulations, rather than a comprehensive survey of loss functions.*

Fully unsupervised and self-supervised training data This is the setting where one only has access to IID samples $g_i \in Y$ from the marginal distribution of g . Such a setting for operator learning without access to ground-truth is the most natural setting in inverse problems since data is the only entity that is always observed. Nevertheless, formulating a fully unsupervised learning problem is not straight-forward.

One possibility in this setting is to consider ‘learning-to-optimise’. Here, the training aims to learn how to accelerate an optimisation solver. Hence, the reconstruction operator $\mathcal{R}: Y \rightarrow X$ is given by handcrafted variational model as in (3) and the aim of the learning is to speed up this solution method. The learning problem is then

$$\hat{\theta} \in \arg \min_{\theta} \mathbb{E}_g \left[\mathcal{L}_Y ((\mathcal{R}_\theta)(g), \mathcal{R}(g)) \right].$$

Clearly, such training can be done without any access to ground-truth solutions.

Another possibility is to consider self-supervised learning. The idea is to use the parametrisation of $\mathcal{R}_\theta: Y \rightarrow X$ as an implicit regulariser by setting up the learning problem

$$\hat{\theta} \in \arg \min_{\theta} \mathbb{E}_g \left[\mathcal{L}_Y ((\mathcal{A} \circ \mathcal{R}_\theta)(g), g) \right] \quad (6)$$

for some loss function $\mathcal{L}_Y: Y \times Y \rightarrow \mathbb{R}$. For the 2-norm this loss would correspond to minimising the data-fidelity and hence care needs to be taken with respect to overfitting noise and considerations of the range of \mathcal{A} .

Remark 4.2. *Note that deep image prior applied to inverse problems often coincides with the above self-supervised learning formulation (6), when only one data sample g is considered. In fact, the learned reconstruction operator \mathcal{R}_θ is expected to fit low-frequency components first, i.e., implicitly regularising, but still requires early stopping or the use of additional regularisers to avoid overfitting noise [21, 28, 50].*

Ground truth examples as training data This is the setting where one only has access to IID samples $f_i \in X$ from the distribution of the ground-truth solutions to the inverse problem, i.e., samples from the true prior. In this setting, one could of course use the forward operator to generate corresponding noisy data $g_i \in Y$, thus recasting the learning problem to a supervised setting, which may represent real measurement data to varying degrees.

A natural approach for setting up a learned reconstruction method that avoids simulated supervised data is to base it on a regulariser that is derived from the original training data, treating $f_i \in X$ as IID samples from the true prior. Many approaches have been based on this typically leveraging deep generative models, e.g., constructing a projection on the range of the pre-trained generator and approximating its inverse. One of the first approaches along these lines was [118] (see also [105]) and many other variants have since then been developed, see e.g. [19, 33, 48, 134, 147].

Unpaired training data This is the setting when training data consists of unpaired IID samples $f_i \in X$ and $g_i \in Y$ from the X - and Y -marginals π_X and π_Y of the joint measure for the $(X \times Y)$ -valued random variable (f, g) , respectively. One can then set up a learning problem that is based on conditional variants of common generative models.

One class of methods are based on training the learned reconstruction operator $\mathcal{R}_{\hat{\theta}}: Y \rightarrow X$ where $\hat{\theta}$ is obtained as

$$\hat{\theta} \in \arg \min_{\theta} \left\{ \mathbb{E}_{\substack{f \sim \pi_X \\ g \sim \pi_Y}} \left[\mathcal{L}_Y \left(\mathcal{A}(\mathcal{R}_{\theta}(g)), g \right) + \mathcal{L}_X \left(\mathcal{R}_{\theta}(g), f \right) \right] + \lambda \mathcal{L}_{\mathcal{P}_X} \left((\mathcal{R}_{\theta})_{\#}(\pi_Y), \pi_X \right) \right\}.$$

In the above, $\mathcal{L}_X: X \times X \rightarrow \mathbb{R}$ and $\mathcal{L}_Y: Y \times Y \rightarrow \mathbb{R}$ are loss functions on X and Y , respectively. Next, \mathcal{P}_X and \mathcal{P}_Y denote the class of probability measures over X and Y , $\mathcal{L}_{\mathcal{P}_X}: \mathcal{P}_X \times \mathcal{P}_X \rightarrow \mathbb{R}$ is a distance notion between probability measures on X , and $(\mathcal{R}_{\theta})_{\#}(\pi_Y) \in \mathcal{P}_X$ denotes the push-forward of the probability measure $\pi_Y \in \mathcal{P}_Y$ by $\mathcal{R}_{\theta}: Y \rightarrow X$. It is common to evaluate $\mathcal{L}_{\mathcal{P}_X}$ using techniques from generative adversarial networks (GANs), which introduce a separate neural operator as discriminator. Finally, the parameter λ controls the balance between the distributional consistency, noise suppression and data consistency. See [39, Section 3] for a survey of various special cases of the above learning problem. One may also consider variants when there is access to a large sample of unpaired data combined with a small amount of paired data, or when parts of the probability distributions involved are known.

On a final note, another common setting in inverse problems is when one has access to a large amount of unsupervised data and a smaller amount of supervised data. One could then consider fine tuning, which is commonly used for re-training a generic foundation model (often a large language model) for a specific task [52, 107, 144].

5 Neural operator architectures

Key considerations in approximating $\mathcal{R}: Y \rightarrow X$ with a neural operator $\mathcal{R}_\theta: Y \rightarrow X$ is to ensure the learned approximation is robust against noise and accurate also for unseen examples. This depends to large extent on the choice of architecture as argued for in Section 5.2. Both accuracy and robustness rely on using an architecture with sufficient model capacity that generalises well and is numerically stable.

Our focus is on learned iterative networks and as outlined in Section 3.2, and more properly described in Section 5.3, these architectures are obtained by unrolling an appropriate iterative scheme. Learned iterative networks are in the scientific literature typically formulated in the finite dimensional setting. The analogous formulation in infinite dimensional setting involves two steps. First is to formulate the iterative scheme in such a setting, and second, to replace the neural networks used in the unrolled scheme with corresponding neural operators. The first step is often straightforward, so formulating learned iterative networks in infinite dimensional setting almost always reduces to finding infinite dimensional analogues of the neural networks used in the unrolled scheme. An example that illustrates this is [12], which considers the functional analytic version of the learned iterative network in [5] (a primal-dual architecture) by replacing the CNNs with differential operators. Likewise, [128] view a neural ordinary differential equation (ODE) as the functional analytic version of the same architecture.

In conclusion, the key part in formulating neural operator variants of learned iterative networks lies in finding infinite dimensional analogues of common neural networks, which will be discussed next.

5.1 Functional analytic versions of common neural network architectures

There has been much interest in extending various neural network architectures to a functional analytic setting. The approaches differ in how they design the layer, i.e., how they extend the combination of affine transformations and non-linear activations to the functional analytic setting. One of the first publications in this direction is [42] that considers approximating non-linear continuous functionals and operators by neural operators. The aim is to use such neural operators in identifying dynamical systems. Another line of development towards neural operators was driven by attempts at using numerical methods for differential equations as a blue print for neural network architectures. Most of the development of neural operator architectures has however been driven by the development of data driven methods for solving inverse problems [115] or PDEs [35, 94, 102].

Convolutional neural operators One of the earliest examples of viewing the discrete convolutional layer in a CNN as a discretisation of an operator is [65]. Here, they consider CNN based residual neural networks (ResNets) and the discrete convolutional layers are viewed as discretisations of a differential operator. The ResNet can thereby be seen as a numerical integration method, so a stable numerical integration could serve as a blue print for setting up a stable CNN based ResNet architecture. The approach is further developed in

[129]. This shows that one can extend a CNN to function spaces by viewing convolutional layers as differential operators. Such an approach was adopted in [12] where the aim was to characterise the microlocal canonical relation of the learned iterative network in [5] (learned primal-dual architecture, see Section 7). Specialised architectures for certain inverse problems have also been developed by discretising the involved differential operators in the governing PDE [15].

The need to extend CNN type of architectures to a functional analytic setting was independently considered in the context of solving PDEs. One of the earliest systematic approaches is presented in [86] that introduced the convolutional neural operator for image generation. Here, one replaces the discrete convolutions in a CNN with convolution operators. The activation function can be any non-linear function that is applied pointwise. This generates aliasing errors as it does not necessarily respect any band-limits of the underlying function space. In particular, non-linear activations can generate features at arbitrarily high frequencies. To address this drawback, [123] modulated the application of the activation function so that the resulting outputs fall within desired band-limits. This results in a convolutional neural operator that maps band-limited functions to band-limited functions, thus respecting the continuous-discrete equivalence which is important when solving PDEs.

A functional analytic version of the U-Net architecture was proposed in [45], showing increased performance over its discrete counterpart in many imaging applications and wrapped with theoretical guarantees around its performance and robustness. Another approach views a U-Net as a one-step unrolling an operator-splitting algorithm that solves some control problem [139].

On a final note, the FNO introduced in [99] can be seen as a neural operator variant of a CNN that uses the Fourier space parametrisation of a convolution.

Transformers The attention mechanism in the transformer architecture has, since its introduction in [22], found widespread use on various applications. A key feature has been its ability to significantly enhance model performance and generalization by offering a mechanism for capturing long range dependencies.

One of the first extensions of transformer architectures to operator learning came in [38] with the introduction of the GK-Transformer. The attention mechanism is here viewed as an integral transform with a learnable kernel (which differs from the FNO that uses a fixed kernel). Input and output features of the GK-Transformer need to have the same discretisation, thus preventing its use in problems where discretisations may vary. Addressing this drawback led to the development of the general neural operator transformer (GNOT) [67]. This is a neural operator architecture capable of accommodating multiple input functions, irregular grids, and multi-scale problems with high flexibility, allowing input and output at any location. See also [135] for similar approach for defining a neural operator based on Fourier type-linear attention.

Finally, one can also consider neural operator architectures in which the attention is represented by a kernel integral operator [36, 93].

5.2 Need for domain adaptation

Machine learning methods, and in particular those based on deep learning, are commonly adapted to a specific domain by choosing appropriate training and

test data, whereas architectures are chosen to be fairly general. In case of operator learning, generic architectures, like those based on CNNs or transformers that make up foundation models and large language models (LLMs), quickly become unfeasible to set-up and train due to the large-scale nature of operator approximation. This *scalability* challenge is especially prominent when deep learning is used to solve inverse problems arising in imaging. In addition, approaches based on generic architectures tend to *generalise poorly* even if trained against very large data sets. Below we illustrate these challenges for image reconstruction in tomography.

Scalability: There has been a few attempts at training neural networks with task agnostic architectures, like AUTOMAP [154], which involves fully connected layers to approximate the inverse operator. An issue with such architectures is that they scale poorly. This is evident already for small 2D tomographic imaging problems, like recovering a 512×512 pixel image from parallel beam tomographic data gathered from 128 different projection angles with a 512 pixel line detector. The first two layers of the AUTOMAP has for this problem $128 \times 512^3 + 512^4 \approx 8.5 \cdot 10^{10}$ parameters, which implies >340 Gigabytes of GPU memory [30]. ETER-net [117], which is a further development of AUTOMAP, does reduce the required parameters by over 80% (by replacing the fully connected/convolutional auto-encoder architecture in AUTOMAP with a recurrent neural network architecture). However, this still means one has a network with about $6.8 \cdot 10^{10}$ parameters that need to be trained.

A similar “back of the envelope” calculation for clinical 3D tomography indicates that using AUTOMAP type of architectures, or some other foundation model based on a generic LLM, results in a network with about 10^{16} learnable parameters. There is not enough training data for learning that many parameters in a reliable way.

Generalisation: A deep learning based approach for tomographic image reconstruction needs to generalise well across variations in instrumentation and data acquisition protocols. Domain agnostic architectures generalise poorly as shown in [13] for the case of AUTOMAP.

The above clearly outlines the drawbacks that comes with using generic neural operator architectures for tomographic image reconstruction. In contrast, the same task can be performed reliably with a learned iterative network that has only about 10^5 (in 2D) and 10^8 (in 3D) learnable parameters [127]. Despite having far less parameters, this learned iterative network also yields state-of-the-art results, is numerically stable, and it generalises well across reasonable variations in data noise level, instrumentation, and data acquisition protocols even when it is trained against a relatively small data set (data from ~ 200 patients).

5.3 Learned iterative networks

As already mentioned in Section 3.2, learned iterative networks refer to neural operators with architectures that are specifically designed to approximate operators that are defined implicitly through an iterative scheme.

Stated formally, let $\mathcal{R}: Y \rightarrow X$ be the operator we seek to approximate. Next, assume there is an iterative scheme $(f^k)_k \subset X$ generated by handcrafted mappings $\Lambda^k: Y \times X^k \rightarrow X$ (updating operators) such that

$$\mathcal{R}(g) := \lim_{k \rightarrow \infty} f^k \quad \text{where} \quad f^k := \Lambda^k(g, f^0, \dots, f^{k-1}) \quad \text{for any } g \in Y. \quad (7)$$

The initialisation $f^0 \in X$ can be as trivial as setting $f^0 = 0$ for any $g \in Y$. Another common choice is to define it as $f^0 := \mathcal{R}_0(g)$ where $\mathcal{R}_0: Y \rightarrow X$ is some handcrafted operator, such as the adjoint operator or filtered backprojection in CT.

A natural question that arises in using a trained neural operator for approximating \mathcal{R} is to decide upon the type of learning problem. As already mentioned, this depends on the type of training data one has and it involves, among other, choosing a suitable loss function. However, as outlined in Section 5.2, we also need further domain adaptation. In particular, there is an option to use neural operators with architectures that are adapted to this specific setting. This brings us to learned iterative networks.

5.3.1 Unrolling an iterative scheme

Learned iterative networks refer to neural operator architectures that are derived from ‘unrolling’ the iterative scheme in (7). Depending on the underlying iterative scheme, these architectures can be categorised as follows:

- Learned gradient networks (Section 6)
- Learned primal-dual networks (Section 7)
- Higher order and networks for non-linear problems (Section 8)

Below we will present a description of the idea of unrolling in an abstract setting. The reader may consult the above cited sections for descriptions of specific learned iterative networks, see also the surveys [4, 44, 64, 110] for additional information.

To describe unrolling in an abstract setting, consider a target operator that is defined by an iterative scheme as in (7). The first step in unrolling this scheme is to truncate iterates by replacing the limit $k \rightarrow \infty$ with $k = N$. The next step is to replace the handcrafted updating operators $\Lambda^k: Y \times X^k \rightarrow X$ in the truncated scheme with neural operators. This results in a learned reconstruction operator $\mathcal{R}_\theta: Y \rightarrow X$ that is defined by the following finite recursive scheme:

$$\mathcal{R}_\theta(g) := f^N \quad \text{where} \quad \begin{cases} f^0 := \mathcal{R}_0(g) \\ f^k := \Lambda_{\theta_k}^k(g, f^0, \dots, f^{k-1}) \quad \text{for } k = 1, \dots, N. \end{cases} \quad (8)$$

Here $\theta := (\theta_1, \dots, \theta_N)$ are the network parameters, $\mathcal{R}_0: Y \rightarrow X$ is the initialisation, and each

$$\Lambda_{\theta_k}^k: Y \times X^k \rightarrow X \quad \text{for } k = 1, \dots, N$$

is a neural operator with its own weights. A natural special case is to use neural operators with fixed architectures at each iteration. In this case we will omit the upper index and write $\Lambda_{\theta_k}^k = \Lambda_{\theta_k}$. Additionally, one can consider weight

sharing, i.e., each network also has the same weights $\Lambda_{\theta_k} = \Lambda_\theta$, but this is not assumed beforehand. Finally, it is also common to further mimic the structure of an iterative scheme by considering residual architectures for computing f^k in (8), i.e.,

$$f^{k+1} := f^k + \Lambda_{\theta_k}^k(g, f^0, \dots, f^{k-1}) \quad \text{for } k = 1, \dots, N. \quad (9)$$

Remark 5.1. *It is important to note that the formulation of the reconstruction operator in (8) is kept abstract on purpose and as such is independent of learning problem or discretisation. This allows now to use any of the loss functions discussed in Section 4 or network components in Section 5.1.*

5.3.2 Historical account of learned iterative networks

The idea of using an iterative scheme as a blue print for a network architecture can be traced back to [61], which considers the case of learning-to-optimise, i.e., training a neural network so that it approximates an optimisation solver. Hence, the target operator maps an objective to its minimiser. More precisely, the focus in [61] is on objective functions that arise in sparse coding. It is therefore natural to consider a proximal gradient method as the iterative scheme, like the iterative shrinkage and thresholding algorithm (ISTA). Using ISTA as a blue print for a CNN-type of neural network is based on the observation that each ISTA iteration consists of a linear operation followed by a non-linear soft-thresholding (proximal to the ℓ_1 -functional). The latter mimics a rectified linear unit (ReLU) activation, so one can assemble a neural network by stacking a finite number of layers where each layer corresponds to an ISTA iterate in which the soft-thresholding has been replaced by ReLU activation. Additionally, deploying weight sharing across the layers results in a recurrent neural network (RNN) type of architecture henceforth called learned iterative shrinkage and thresholding algorithm (LISTA).

Learned iterative networks that were obtained by unrolling (unfolding) a truncated iterative scheme can also be trained in supervised manner to solve an ill-posed inverse problem. One of the earliest examples of this was for blind deconvolution [133]. Another inverse problem is 2D tomographic image reconstruction. The possibility to use learned iterative networks, like LISTA, for this inverse problem is mentioned in [82]. However, the paper does not implement such an architecture. Instead, it moves on to observe that the normal operator $\mathcal{A}^* \mathcal{A}$ in this setting is a convolution type operator, i.e., it is smoothing of order 1, which follows from the fact that \mathcal{A} is the ray transform. Hence, a single LISTA layer has the form of a filtering followed by pointwise non-linearity. This in turn serves as a motivation for a post-processing based approach in which a U-Net is trained to improve upon filtered back-projection (FBP) reconstructions (FBPConvNet), i.e., the LISTA architecture is merely used as a way to motivate the use of U-Net as a post-processing step. The first example of using a learned iterative method for solving more general inverse problems, including deconvolution and tomographic image reconstruction, appeared in [6]. The architecture here is given by unrolling a gradient descent scheme for minimising a differentiable objective representing a penalised (regularised) least-squares fidelity term. The forward operator is here replaceable in a plug-and-play manner. Such a network was then trained end-to-end for 2D tomographic image reconstruction.

It is also worth mentioning early work on recurrent inference machines that dates back to 2015¹. This work, which later appeared as a pre-print [121], essentially considers a learned iterative network for performing various linear image processing tasks. The examples given are image denoising and super-resolution. The reader may also consult [110, Table 1] that lists publications where learned iterative networks are used for performing various signal and image processing tasks.

In conclusion, it is important to note that a learned iterative network is merely a choice of neural network architecture. Which task one seeks to perform with such a neural network depends to large extent on how it is trained. Hence, the choice of learned iterative networks is more about *how to compute* rather than *what to compute*. Many learned reconstruction methods with a learned iterative network are trained end-to-end against supervised data. The unrolling is often based on an iterative scheme that in the limit yields a minimiser to a penalised least-squares solution to the inverse problem. An unfortunate consequence of this is that many papers erroneously claim that more unrolled iterates yield a better approximation to the minimiser. Without further assumptions, the correct interpretation is that unrolling more iterates only increases the model capacity of the network.

6 Learned Gradient Networks

Learned gradient networks are learned reconstruction operators, which are specifically designed to approximate reconstruction operators $\mathcal{R}: Y \rightarrow X$ based on iterative gradient based schemes. Examples are operator that compute minimiser to a convex differentiable objective, another example is to compute a regularised solution of an ill-posed inverse problem. In other words, these are the learned iterative networks which are obtained by unrolling a gradient based optimisation scheme.

The starting point in constructing a learned gradient network is to specify a *variational model* for the operator \mathcal{R} that one seeks to approximate. Assume here that one can define this operator implicitly by a variational problem that seeks to minimise a differentiable cost functional $\mathcal{E}_g: X \rightarrow \mathbb{R}$ for given $g \in Y$:

$$\mathcal{R}(g) := \arg \min_{f \in X} \mathcal{E}_g(f) \quad \text{for } g \in Y. \quad (10)$$

Next, consider a gradient descent scheme for computing a minimiser in (10). Such a scheme for given $g \in Y$ reads as

$$\begin{cases} f^0 := \mathcal{R}_0(g) \\ f^k := f^{k-1} - \omega_k \nabla \mathcal{E}_g(f^{k-1}) \quad \text{for some } \omega_k > 0 \text{ and } k = 1, 2, \dots \end{cases} \quad (11)$$

If the cost functional $f \mapsto \mathcal{E}_g(f)$ is also convex, then the sequence $(f^k)_k \subset X$ in (11), which depends on g , can be used to evaluate \mathcal{R} , since $\mathcal{R}(g) = \lim_{k \rightarrow \infty} f^k$. *Learned gradient networks* now seek to formulate a neural operator architecture by combining the updates in (11) with data driven components as in (8). In the following we will first discuss an illustrative example and then survey common approaches to obtain such networks.

¹<https://openreview.net/forum?id=HkSOIP9lg>

Adaptation to inverse problems Following the underlying paradigm of this chapter, we now adapt the gradient scheme in (11) to the domain of inverse problems. Namely, we introduce more structure to the general minimisation problem (10) by aiming to compute a solution to the operator equation (2). We will also restrict this section linear forward operators $\mathcal{A}: X \rightarrow Y$, the case when \mathcal{A} is non-linear is discussed in Section 8.

The original use case for solving ill-posed inverse problems was to approximate reconstruction operators that are defined as minimisers to objectives $\mathcal{E}_g: X \rightarrow \mathbb{R}$ of the form

$$\mathcal{E}_g(f) := \mathcal{Q}_g(f) + \mathcal{S}(f) \quad \text{for } f \in X. \quad (12)$$

Here, $\mathcal{Q}_g: X \rightarrow \mathbb{R}$ depends on g and $\mathcal{S}: X \rightarrow \mathbb{R}$ is the regulariser. The former is commonly given by a loss in Y using the knowledge of \mathcal{A} as

$$\mathcal{Q}_g(f) := \mathcal{L}_Y(\mathcal{A}f, g) \quad \text{for } f \in X. \quad (13)$$

where $\mathcal{L}_Y: Y \times Y \rightarrow \mathbb{R}$ is a data-fidelity term, often given as suitable norm. The explicit regulariser $\mathcal{S}: Y \rightarrow \mathbb{R}$ is often omitted in learned iterative networks and replaced by the learned components. We will get back to this in the remainder of this section.

Thus, to illustrate the concept of learned iterative networks let us consider a special case that is often of interest. Namely, when the objective $\mathcal{E}_g: X \rightarrow \mathbb{R}$ in (12) only consists of the data-fidelity, i.e., $\mathcal{E}_g(f) := \mathcal{Q}_g(f)$. As discussed earlier, if $f \mapsto \mathcal{Q}_g(f)$ is differentiable, then one can find a local minima by a gradient descent scheme:

$$f^k := f^{k-1} - \theta_k \nabla \mathcal{Q}_g(f^{k-1}) \quad \text{for } k = 0, 1, 2, \dots, \quad (14)$$

where ∇ is the X -gradient w.r.t. the f -variable. A common setting is when the data-fidelity \mathcal{L}_Y is the squared Y -norm, i.e., $\mathcal{L}_Y(h, g) := \frac{1}{2} \|h - g\|_Y^2$. Then

$$\mathcal{Q}_g(f) = \frac{1}{2} \|\mathcal{A}f - g\|_Y^2, \quad (15)$$

so the gradient $\nabla \mathcal{Q}_g: X \rightarrow X$ is given as

$$\nabla \mathcal{Q}_g(f) = \mathcal{A}^*(\mathcal{A}f - g) \quad \text{for } f \in X. \quad (16)$$

The iterates in (14) will then coincide with Landweber iterations and represent a special case of (8) with an updating rule of the form

$$f^k = \Lambda_{\theta_k}(f^{k-1}, \nabla \mathcal{Q}_g(f^{k-1})) := f^{k-1} - \theta_k \nabla \mathcal{Q}_g(f^{k-1}),$$

which can be seen as a gradient descent (Landweber) step with a learnable step-size θ_k . Now, this can readily be generalised to the general form (8) by using neural operators for Λ_{θ_k} within the update rules, where the parameters θ_k are high-dimensional, instead of a scalar step-size.

Using suitably chosen neural operators $\Lambda_{\theta_k}: X \times X \rightarrow X$ as the *neural updating operator* provides the standard form of a *learned gradient network* as in [6]. This yields the learned reconstruction operator $\mathcal{R}_\theta: Y \rightarrow X$ with $\theta := (\theta_1, \dots, \theta_N)$ that is defined as

$$\mathcal{R}_\theta(g) := f^N \quad \text{where} \quad f^k = \Lambda_{\theta_k}(f^{k-1}, \nabla \mathcal{Q}_g(f^{k-1})) \quad \text{for } k = 1, \dots, N. \quad (17)$$

Here, $f^0 \in X$ is an initialisation, either given by $f^0 = \mathcal{R}_0(g)$ where \mathcal{R}_0 is some handcrafted reconstruction method, $f^0 = \mathcal{A}^* g$, or $f^0 = 0$. We will discuss such learned gradient networks further in Section 6.1.1 with a specific focus on least-squares data-fidelity terms.

The neural updating operators The learned reconstruction operator in (17) is a neural operator with an architecture of the form (8) without memory. The neural updating operators are defined as mappings $\Lambda_{\theta_k}: X \times X \rightarrow X$ on X only and their architecture does not involve data or the forward operator (or its adjoint). These only enter into the evaluation of the gradient $\nabla \mathcal{Q}_g(f)$.

This structure of the neural updating operators also illustrates how learning is intertwined with handcrafting the inputs to the network. In fact, many learned iterative networks are variants of (17) with specific form on the neural updating operators:

$$\Lambda_\theta(f, \nabla \mathcal{Q}_g(f)) := f - \nabla \mathcal{Q}_g(f) + \Gamma_\theta(f) \quad (\text{variational networks}) \quad (18)$$

$$\Lambda_\theta(f, \nabla \mathcal{Q}_g(f)) := \Gamma_\theta(f - \nabla \mathcal{Q}_g(f)) \quad (\text{learned proximal gradient}) \quad (19)$$

In the above, $\Gamma_\theta: X \rightarrow X$ is a neural operator representing the learned aspect of the updates, whereas the other components are handcrafted.

When applying the above methods to inverse problems in imaging, note that in particular all neural operators are mappings from X to X , e.g., images to images. Hence, learned iterative networks stack a sequence of such image-to-image transforms using couplings that involve handcrafted components through the update direction $\nabla \mathcal{Q}_g(f)$. Additionally, the neural update operators Λ_{θ_k} are usually not very expressive as we will discuss in the following subsections. This can be intuitively understood by realising that the update directions $\nabla \mathcal{Q}_g(f)$ encode non-local relations through the involvement of the forward operator (and its adjoint), thus the learned network component primarily learns local interactions. Consequently, very deep and expressive networks that can learn long range relations may not be needed. Nevertheless, this statement needs to be taken with care and is highly dependent on the application as well as the ability of the update direction $\nabla \mathcal{Q}_g(f) \in X$ to encode the needed long range relations.

6.1 Classes of learned gradient networks

As discussed above, learned gradient networks for approximating \mathcal{R} are obtained by unrolling the gradient descent scheme in (11). This can be done in many ways, but the overall procedure is to first truncate the scheme to N iterates, then replace the updates at each iterate with neural updating operators $\Lambda_{\theta_k}: X \times X \rightarrow X$. This yields a learned reconstruction operator $\mathcal{R}_\theta: Y \rightarrow X$ with $\theta := (\theta_1, \dots, \theta_N)$ that is defined as

$$\mathcal{R}_\theta(g) := f^N \quad \text{where} \quad \begin{cases} f^0 := \mathcal{R}_0(g) \\ f^k := \Lambda_{\theta_k}(f^{k-1}, \nabla \mathcal{E}_g(f^{k-1})) \quad \text{for } k = 1, \dots, N. \end{cases} \quad (20)$$

One often uses residual architectures for the neural update operators in (20), which yields the residual update structure as variant of (9):

$$f^k := f^{k-1} + \Lambda_{\theta_k}(f^{k-1}, \nabla \mathcal{E}_g(f^{k-1})). \quad (21)$$

In the following we will discuss three specific choices to introduce more structure into the updates (20).

6.1.1 Learned least squares networks

Let us first discuss the standard learned least squares network (17) further based on [6]. Here the gradient updates are given by the gradient of the squared data-fidelity (16). The learned reconstruction operator is then given as $\mathcal{R}_\theta(g) := f^N$ where $\theta = (\theta_1, \dots, \theta_N)$ and

$$\begin{cases} f^0 := \mathcal{R}_0(g) \\ f^k := \Lambda_{\theta_k} \left(f^{k-1}, \mathcal{A}^* (\mathcal{A} f^{k-1} - g) \right) \quad \text{for } k = 1, \dots, N. \end{cases} \quad (22)$$

In the above variant the neural update operator $\Lambda_{\theta_k} : X \times X \rightarrow X$ receives only two inputs, the current iterate f^{k-1} as well as the gradient information. The original implementation in [6] additionally used a memory of m previous iterates and a handcrafted regulariser as the input to the network, that is the update becomes

$$\begin{cases} f^k := 0 & \text{if } k < 0, \\ f^k := \Lambda_{\theta_k} \left(f^{k-1-m}, \dots, f^{k-1}, \mathcal{A}^* (\mathcal{A} f^{k-1} - g), \nabla \mathcal{S}(f^{k-1}) \right) & \text{if } k \geq 0, \end{cases} \quad (23)$$

where $\mathcal{S} : X \rightarrow \mathbb{R}$ was the Dirichlet energy as in classical Tikhonov regularisation. However, it should be noted that further experiments in the supervised setting showed that using an explicit regulariser in the updates is not necessary for improving the reconstruction quality. In fact, an additional explicit regulariser will modify the neural network architecture, but it is unclear in which way this may impact the regularising properties of the learned gradient network for solving ill-posed inverse problems. Instead, the common approach is to assume that the prior information and regularising effect is implicitly contained in the training data. On the other hand, the memory in (23) can improve reconstructions slightly and helps to stabilise the training.

Implementation The formulation presented in (22) leaves the freedom to choose suitable parametrisations for neural operator Λ_θ to realise the mapping between the spaces $X \times X \rightarrow X$. This choice largely depends also on the discretisation of X , that means, if we treat X as a function space, then a neural operator such as FNOs are a suitable choice. Whereas, for classic discretisations in $\mathbb{R}^{n \times n}$ it is common to apply a CNN or related architectures.

For example, the original implementation presented in [6] is using a CNN. The updates follow a residual formulation as in (21), where each neural network Λ_{θ_k} is a simple 3-layer CNN with 32 channels. It should be noted, that this architectural choice is similar to ResNet architectures [74]. A total number of $N = 10$ iterations was trained using a fully supervised loss.

Remark 6.1. *While the use of the forward operator \mathcal{A} is essential for domain adaptation and allows for the use of smaller networks, it introduces a large computational overhead to the training. Additionally, this also necessitates the use of specialised scientific software for the evaluation of \mathcal{A} and can provide a conceptual challenge. We will discuss these aspects further in Section 9.*

Choice of learning problem and training regime With the learned reconstruction operator given, one now can design a suitable learning problem according to the training data given, as outlined in Section 4. Specifically, that means any of the loss functions are possible conceptually. Nevertheless, most commonly the learned reconstruction operator \mathcal{R}_θ is trained trained end-to-end given supervised training data $\{f_i, g_i\} \in X \times Y$ by minimising the empirical loss

$$\hat{\theta} = \arg \min_{\theta \in \Theta} \sum_i \mathcal{L}_X(\mathcal{R}_\theta(g_i), f_i), \quad (24)$$

as earlier discussed introduced in (5). Computationally, this can be demanding, as it requires evaluation of the update directions, including the forward model \mathcal{A} and computation of \mathcal{A}^* in each forward as well as backward pass N -times, that is $4N$ operator evaluations for each training iteration, which will be well in the order of ten thousands.

Thus, training of the learned reconstruction operator \mathcal{R}_θ can pose a major computational challenge. Particularly, in case the operator \mathcal{A} is computationally demanding, e.g., evaluation times larger than a second, different training regimes are necessary to train the reconstruction operator \mathcal{R}_θ . One such option as a greedy training approach to avoid the computational demanding evaluation in each training iteration [9, 73]. Instead of the end-to-end loss function above, only iterate-wise optimality is required, thus the terminology greedy; alternatively this may also be called sequential training. For the reconstruction operator in (22), this leads to N sequential training problems of the form

$$\hat{\theta}_k \in \arg \min_{\theta \in \Theta} \sum_i \mathcal{L}_X\left(\Lambda_{\theta_k}\left(f_i^{k-1}, \mathcal{A}^*(\mathcal{A} f_i^{k-1} - g_i)\right), f_i\right), \quad (25)$$

to obtain the final trained $\mathcal{R}_{\hat{\theta}}$ with $\hat{\theta} = \{\hat{\theta}_1, \dots, \hat{\theta}_N\}$. For each training in (25) we assume that the previous neural update operator $\Lambda_{\hat{\theta}_{k-1}}$ for iteration $k-1$ has been trained. Then one can evaluate f_i^{k-1} with the fixed network parameters $\hat{\theta}_{k-1}$ by

$$f_i^{k-1} := \Lambda_{\hat{\theta}_{k-1}}\left(f_i^{k-2}, \mathcal{A}^*(\mathcal{A} f_i^{k-2} - g_i)\right).$$

Additionally, the gradients $\mathcal{A}^*(\mathcal{A} f_i^{k-1} - g_i)$ needed for (25) can be pre-computed for all training pairs. Note, that for $k = 1$ only the gradient for the initialisation f^0 is computed. This greedy procedure allows decoupling of the network training from the evaluation of the model components and enables efficient training even for computationally demanding inverse problems, such as 3D photoacoustic tomography [73], where the evaluation of the forward operator takes more than 10 seconds, or in astronomical imaging [9].

Note that the same learned reconstruction operator \mathcal{R}_θ can be trained either end-to-end (24) or with a greedy scheme (25), but the resulting parameters $\hat{\theta}$ will be different. In fact, the greedy loss represents an upper bound on optimality of parameters to the end-to-end loss. We will discuss further examples of approaches to manage the computational burden in Section 9.

6.1.2 Learned proximal networks

The learned least squares network in the previous section is based on the variational model in (10) with a cost functional of form (12), where the neural

updating operator does not make use of further structure apart from the use of gradient information of the cost functional \mathcal{E}_g . Next we will introduce such further structure with *learned proximal networks*.

Here, the motivation is to improve upon interpretability and generalisation properties. The guiding principle in learned proximal networks is to make use of the structure that is offered by forward-backward splitting, also called proximal gradient descent schemes. Such networks are specifically designed for approximating operators $\mathcal{R}: Y \rightarrow X$ that are defined by a variational model (10) in which the cost functional $\mathcal{E}_g: X \rightarrow \mathbb{R}$ for data $g \in Y$ has the form in (12):

$$\mathcal{E}_g(f) = \mathcal{Q}_g(f) + \mathcal{S}(f) \quad \text{with} \quad \mathcal{Q}_g(f) := \mathcal{L}_Y(\mathcal{A}f, g). \quad (26)$$

Here, $\mathcal{L}_Y: Y \times Y \rightarrow \mathbb{R}$ (data-fidelity), $\mathcal{A}: X \rightarrow Y$ (forward operator), and $\mathcal{S}: X \rightarrow \mathbb{R}$ (regulariser) are all handcrafted.

If $\mathcal{Q}_g(f): X \rightarrow \mathbb{R}$ is convex and differentiable and \mathcal{S} is convex, but not necessarily differentiable, then one can evaluate $\mathcal{R}: Y \rightarrow X$ using the mentioned forward-backward splitting (proximal gradient descent scheme). Then we get $\mathcal{R}(g) = \lim_{k \rightarrow \infty} f^k$ where the sequence $(f^k)_k \subset X$ is generated as

$$\begin{cases} f^0 := \mathcal{R}_0(g), \\ f^k := \text{prox}_{\mathcal{S}}(f^{k-1} - \omega_k \nabla \mathcal{Q}_g(f^{k-1}, g)), \quad \text{for } k = 1, 2, \dots \end{cases} \quad (27)$$

for some suitable choice $\omega_k > 0$ and initialisation $\mathcal{R}_0: Y \rightarrow X$. In the above, the functional $\text{prox}_{\mathcal{S}}: X \rightarrow \mathbb{R}$ is the proximal operator defined as

$$\text{prox}_{\mathcal{S}}(f) := \arg \min_{u \in X} \|u - f\|_2^2 + \mathcal{S}(u) \quad \text{for } f \in X. \quad (28)$$

This can be interpreted as denoising of the input $f \in X$ with respect to \mathcal{S} and thereby projection it onto the admissible set defined by the regulariser \mathcal{S} .

The scheme in (27) separates the iterative procedure into two steps, one explicit gradient step with respect to the data-fidelity followed by the proximal operator. Since the proximal operator enforces the regulariser, which contains prior knowledge on the reconstructions, it is now straight-forward to replace it by a learned component. This leads to the more structured *learned proximal network* where the neural operator $\mathcal{R}_\theta: Y \rightarrow X$ with $\theta = (\theta_1, \dots, \theta_N)$ is given as $\mathcal{R}_\theta(g) := f^N$ where

$$\begin{cases} f^0 := \mathcal{R}_0(g) \\ f^k := \Lambda_{\theta_k}(f^{k-1} - \omega_k \nabla \mathcal{Q}_g(f^{k-1})) \quad \text{for } k = 1, \dots, N. \end{cases} \quad (29)$$

Further structure from (27) can be included into the above architecture by requiring to use same weights for all unrolled iterates (20) (weight-sharing). Then, the updating operator Λ_θ has the same parameters for each iterate, so the architecture of the resulting learned proximal network with weight-sharing is given by

$$f^k := \Lambda_\theta(f^{k-1} - \omega_k \nabla \mathcal{Q}_g(f^{k-1})). \quad (30)$$

Weight-sharing reduces expressive power of the architecture, but it may improve upon interpretability. In fact, learned proximal networks with weight-sharing can be interpreted as including one more layer of structure as it allows to make

connections to a fixed proximal operator for the regulariser \mathcal{S} . Nevertheless, if no constraints on the parameter space Θ are made, then there is no guarantee that the learned updating operator Λ_θ corresponds to a proximal operator for some regulariser. Finally, weight-sharing allows to perform more iterations than the fixed amount of N . This specifically is the basis for some theoretical results we will discuss in the following.

Implementation Both reconstruction operators in (29) and (30) can be trained in the same way as the previously discussed least squares networks. That means, depending on the type of training data, a fully supervised or semi- and unsupervised setting is possible. The same limitations on computational cost of the involved forward operator apply for the proximal networks.

Additionally, we can now exploit the structure in (30) further by introducing constraints on the updating operator Λ_θ . This allows us to obtain two popular approaches in the literature, plug-and-play (PnP) schemes and deep equilibrium (DEQ) networks. We note, that these two approaches originate from the same formulation of the reconstruction operator \mathcal{R}_θ in (30), but offering distinctive training advantages as well as theoretical results which we will discuss next.

Relation to plug-and-play (PnP) schemes While PnP schemes are considered a separate research direction to unrolling schemes, we like to make the connection here from the viewpoint of learned iterative schemes and a learned reconstruction operator. For us the difference between PnP and unrolling lies in the choice of learning problem, as we will see shortly, and not in the formulation of the learned reconstruction operator.

Let us first point out the differences between unrolling and PnP schemes. In particular, there are two main primary distinctions. First, PnP methods separate the training of the network component $\Lambda_\theta : X \rightarrow X$ from the iterative algorithm, i.e., a different learning problem. Second, conventionally unrolling schemes require truncated iterations, whereas PnP schemes consider the formulation in (27) to formulate the learned version (30) to allow for a convergence analysis in the limit. That means we could say that unrolling schemes consider $\mathcal{R}_\theta(g) = f^N$ versus $\mathcal{R}_\theta(g) = f^\infty$ for PnP. Note, that in practice we still have to truncate in the latter case, but at an assumed point of convergence. We will summarise here only shortly some underlying theory and refer to [70, 84, 113] for further details.

The viewpoint of plug-and-play schemes originates from the insight that the proximal operator (28) in the updates (27) performs a denoising of the input. Thus, it may be replaced by a generic denoiser [142] which eliminates Gaussian noise. This relates to the first distinction mentioned above, which now allows for training of the neural operator Λ_θ as a Gaussian denoiser. That is, training pairs are given as samples in X only, i.e., $\{f_i, \tilde{f}_i\}_i$, with $\tilde{f} = f + e$ where e is zero-mean Gaussian noise. In Inverse problems, the noisy realisation of f may be also obtained from the measurements g with a handcrafted reconstruction operator, such that $\tilde{f} = \mathcal{R}(g)$, if it preserves Gaussian noise. Nevertheless, it should be noted that for many inverse problems the reconstructed image \tilde{f} does contain artefacts and noise that is not purely zero-mean Gaussian, especially so if an undersampled problem is considered, e.g., sparse or limited-angle X-ray tomography. This is one of the primary limitations of PnP schemes for inverse

problems and hence PnP schemes are mostly successful for fully-sampled inverse problems and have limited success for severely ill-posed or undersampled cases. Some recent advances have been made to extend PnP schemes to Poisson data [78, 89].

On the other hand, and with respect to the second distinction, since the proximal operator in the classic iterative scheme has been replaced, one can examine the limiting case and establish convergence results of varying degree. For instance, we observe that if the iterative update given by the mapping $\Lambda_\theta: f^{k-1} \mapsto f^k$ is contractive, then the iterative process of applying Λ_θ repeatedly will converge to a fixed-point f^∞ with

$$\lim_{k \rightarrow \infty} \Lambda(f^k) = \Lambda(f^\infty) = f^\infty. \quad (31)$$

This requires, that the networks Λ_θ in composition with the iterative procedure $f^{k-1} - \omega \nabla \mathcal{Q}_g(f^{k-1})$ are contractive. Conditions on the step-length, networks, and operators have been established in various settings [41, 130] and generally require to constrain the Lipschitz constant of the network Λ_θ together with an appropriate step-size choice for ω . Finally, stronger results can be achieved by further restricting the network. For instance, objective convergence [79, 114], or a convergent regularisation method [51, 70]. Finally, it should be said that while strong theoretical results can be achieved by restricting the networks and as such the parameter space, this will lead to less expressive networks and most commonly will result in deteriorated quantitative performance.

To summarise, for a learned reconstruction operator $\mathcal{R}_\theta(g) = f^N$ the PnP framework offers an alternative learning problem to effectively train the neural updating operator Λ_θ with only data on X . Computationally, this is even cheaper than the greedy training in (25), since no operator evaluation is involved in the training. Nevertheless, the PnP theory only holds, when a reconstruction operator $\mathcal{R}_\theta(g) = f^\infty$ is considered.

Deep equilibrium (DEQ) networks Starting from (30) and consider again a learned reconstruction operator in the limit $\mathcal{R}_\theta(g) = f^\infty$, and assuming that the iterates converge to a fixed point (31). The difference for DEQ networks is that in fact an unrolled algorithm is trained, which means here that the forward pass of the reconstruction operator (29) is evaluated in the loss function. Clearly, while we cannot evaluate the limit we can make use of the fixed point formulation to compute the gradients for training as we will outline next shortly.

We assume that the learned reconstruction operator $\mathcal{R}_\theta: Y \rightarrow X$ iteratively applies the neural updating operator $\Lambda_\theta: X \rightarrow X$ and that $\mathcal{R}_\theta(g) = f^\infty$ is a fixed point with $\Lambda_\theta(f^\infty) = f^\infty$ as in (31). Given the loss function $\mathcal{L}_X: X \times X \rightarrow \mathbb{R}$ with

$$\mathcal{L}_X(\mathcal{R}_\theta(g), f) = \mathcal{L}_X(f^\infty, f),$$

we differentiate with respect to the network parameters using chain rule

$$\frac{\partial \mathcal{L}_X(\mathcal{R}_\theta(g), f)}{\partial \theta} = \frac{\partial \mathcal{L}_X(\mathcal{R}_\theta(g), f)}{\partial \mathcal{R}_\theta(g)} \frac{\partial \mathcal{R}_\theta(g)}{\partial \theta}. \quad (32)$$

The first term is simply the loss function differentiated with respect to the reconstruction. For the standard least squares loss and using the fixed point

$\mathcal{R}_\theta(g) = f^\infty$ we obtain

$$\frac{\partial \mathcal{L}_X(f^\infty, f)}{\partial f^\infty} = \frac{\partial \frac{1}{2} \|f^\infty - f\|_2^2}{\partial f^\infty} = f^\infty - f.$$

The second term in (32) can be simplified by using the fixed point formulation $\mathcal{R}(g) = f^\infty = \Lambda_\theta(f^\infty)$. Again, differentiating with respect to the network parameters gives

$$\frac{\partial f^\infty}{\partial \theta} = \frac{\partial \Lambda_\theta(f^\infty)}{\partial \theta} + \frac{\partial \Lambda_\theta(f^\infty)}{\partial f^\infty} \frac{\partial f^\infty}{\partial \theta}$$

and solving for $\partial f^\infty / \partial \theta$ to obtain

$$\frac{\partial f^\infty}{\partial \theta} = \left(\mathcal{I} - \frac{\partial \Lambda_\theta(f^\infty)}{\partial f^\infty} \right)^{-1} \frac{\partial \Lambda_\theta(f^\infty)}{\partial \theta}.$$

Substituting this into (32) we get a short form of the gradient

$$\frac{\partial \mathcal{L}_X(\mathcal{R}_\theta(g), f)}{\partial \theta} = \frac{\partial \mathcal{L}_X(f^\infty)}{\partial f^\infty} \left(\mathcal{I} - \frac{\partial \Lambda_\theta(f^\infty)}{\partial f^\infty} \right)^{-1} \frac{\partial \Lambda_\theta(f^\infty)}{\partial \theta}. \quad (33)$$

As we see, only the first term is loss-function dependent. The second term involves differentiating the network with respect to its input $\frac{\partial \Lambda_\theta(f^\infty)}{\partial f^\infty}$, which amounts to calculating the network Jacobian in practice and can be done via automatic differentiation. Most notably, to compute the loss (33) we do not need to perform backpropagation through all iterates, which reduces memory consumption to train the networks. Nevertheless, the forward pass needs to be evaluated. Thus, this technique primarily allows to reduce the high memory consumption needed for efficient backpropagation, but computational limitations remain for expensive forward operators.

In practice, the fixed point is computed using acceleration techniques to reduce the amount of iterations and a finite number of iterations is considered in training, see [23, 59] for further details. The expensive calculation of the Jacobians in (32) can in fact be simplified as well, most notably using Jacobian free updates [49, 58].

Finally, let us note that PnP and DEQ models share a close connection. Both are based on considering the limiting case $\mathcal{R}_\theta(g) = f^N$ for the theory and not a finite amount of iterates. In both cases, the networks are considered to be contractive, but a crucial difference is that PnP networks are additionally parametrised as denoiser, while DEQ are not further constrained. The former does allow to establish stronger results than fixed point convergence, as discussed earlier. The latter offers computational advantages for applications in limited-angle and or very sparse tomographic settings where artefacts can not be easily described as common noise distributions. In such cases DEQ models show better performance that is closer matched to conventional unrolling schemes [71].

6.1.3 Variational networks & total deep variation

The starting point for *variational networks* follows a similar setup as for learned proximal networks. In particular, also variational networks aim at parametrising the regulariser in a gradient descent scheme. Rather than through the use

of a proximal operator, variational networks parametrise the gradient of the regulariser directly.

The underlying optimisation algorithm for variational networks is a standard gradient descent scheme for minimising $\mathcal{E}_g: X \rightarrow \mathbb{R}$ in (26) for given data $g \in Y$. The data-fidelity functional $\mathcal{Q}_g(f): X \rightarrow \mathbb{R}$, forward operator $\mathcal{A}: X \rightarrow Y$, and regulariser $\mathcal{S}: X \rightarrow \mathbb{R}$ are here handcrafted. For differentiable $\mathcal{Q}_g(f): X \rightarrow \mathbb{R}$ and $\mathcal{S}: X \rightarrow \mathbb{R}$ we can write the standard gradient descent scheme as in (11) by

$$\begin{cases} f^0 := \mathcal{R}_0(g) \\ f^k := f^{k-1} - \omega_k (\nabla \mathcal{Q}_g(f^{k-1}) + \nabla \mathcal{S}(f^{k-1})) \quad \text{for } \omega_k > 0 \text{ and } k = 1, 2, \dots \end{cases} \quad (34)$$

Variational networks keep the gradient descent structure and aim at parametrising the gradient of the regulariser $\nabla \mathcal{S}: X \rightarrow X$ directly. Note, that the gradient of the regulariser maps between the image space X and can be well replaced by a neural network. While, in the original publication [92] a Fields-of-Experts (FoE) model has been used to create an interpretable representation, we will follow here a general formulation using a neural operator for consistency with the previous sections. Thus, let us introduce the iteration dependent neural operator $\Lambda_{\theta_k}: X \rightarrow X$ replacing the gradient of the regulariser for each iteration. The learned reconstruction operator is then given as $\mathcal{R}_\theta(g) := f^N$ where

$$\begin{cases} f^0 := \mathcal{R}_0(g) \\ f^k := f^{k-1} - \omega_k \nabla \mathcal{Q}_g(f^{k-1}) + \Lambda_{\theta_k}(f^{k-1}) \quad \text{for } k = 1, \dots, N. \end{cases} \quad (35)$$

Without introducing further structure in the neural operator Λ_{θ_k} , there are no theoretical guarantees available for the above learned reconstruction operator.

The original paper [92] considered the FoE parametrisation, which allowed to learn activation functions. While it provided some insights into what kind of nonlinear features the network learns, this original parametrisation did not provide any convergence or stability guarantees. Nevertheless, more recent work addressed this by introducing an extended framework as the so-called Total Deep Variation [90, 91] which does provide a stability analysis. We will discuss both approaches in the following.

Remark 6.2. *A theoretical interpretation of (35) in the context of learning-to-optimise can be derived, if the neural operator Λ_θ is fixed for each iteration.*

Original implementation and extensions Variational networks are among the first learned iterative networks and for the time the connection to variational regularisation was the most apparent. Even though theoretically there is only a minor difference to other reconstruction operators based on unrolling schemes, as we will see shortly.

Let us now shortly discuss the original variational networks as proposed by Kobler et al. [66, 92], which take their inspiration from variational regularisation models where the regularisation functional \mathcal{S} is equipped with parametrisations that go beyond handcrafted regularisers such Total Variation (TV). More concretely, variational networks take their inspiration from the FoE model described in [43, 124, 125]. Let us consider here a general FoE parameterisation of the the

regulariser as

$$\mathcal{S}_\theta(f) := \sum_{i=1}^m \left[\sum_{k=1}^n \rho_i((J_i f)_k) \right] \quad \text{with } \theta = (\rho_1, \dots, \rho_m, J_1, \dots, J_m). \quad (36)$$

Here, $J_i: X \rightarrow X^n$ are linear transforms, usually given by a convolution with n filters. m is the number of regularisation functions, with parameterisable non-linear functions $\rho_i: \mathbb{R} \rightarrow \mathbb{R}$.

The updates in (34) require the gradient of the regulariser \mathcal{S}_θ , which can be computed by

$$\nabla \mathcal{S}_\theta(f) := \sum_{i=1}^m J_i^* \rho'_i(J_i f), \quad (37)$$

with the adjoint operator $J^*: X^n \rightarrow X$. Note, that the linear operator J expands the image space and the adjoint J^* collapses it again. This is similar to a two layer neural network, where the filters are tied together.

From here, we obtain the associated reconstruction operator for variational networks [66, 92] as $\mathcal{R}_\theta(g) := f^N$ with

$$\begin{cases} f^0 := \mathcal{R}_0(g) \\ f^k := f^{k-1} - \omega_k \nabla \mathcal{Q}_g(f^{k-1}) + \nabla \mathcal{S}_{\theta_{k-1}}(f^{k-1}) \quad \text{for } k = 1, \dots, N, \end{cases} \quad (38)$$

where now each iterate has its own set of parameters. The training of the reconstruction operator is performed fully supervised and end-to-end. The first paper by Kobler et al. [92] also suggests to parameterise the data-fidelity term \mathcal{Q}_g in a similar manner to (36), later developments [66] have omitted the learned component on the data-fidelity.

Despite the name variational networks, the connection to variational methods is restricted to parametrising the learned update from a FoE perspective. Training the reconstruction operator supervised and with changing weights in each iteration removes the possibility to interpret \mathcal{R}_θ as a minimiser of a variational cost functional.

Finally, since the connection to a minimiser of a variational cost functional is not satisfied, it has been easy to replace the learned component by a general neural operator as in our formulation (35). This offers to use larger and more expressive networks for $\Lambda_\theta: X \rightarrow X$, such as U-Nets.

Total Deep Variation The framework of variational networks has been extended to include multi-scale networks, likely inspired by the popular U-Net architecture, introduced as total deep variation (TDV) in [90, 91]. Additionally, the work establishes robustness and stability results with respect to input as well as learned parameters based on a mean-field optimal control interpretation. That is, the formulation of the reconstruction operator is based on a continuous-in-time gradient flow rather than a discrete iterative process. One can then formulate the reconstruction operator $\mathcal{R}_\theta: Y \rightarrow X$ that assigns the reconstruction at finite time $T > 0$, i.e., $\mathcal{R}_\theta(g) = f(T)$. Similar to variational networks the gradient flow is defined to minimise a variational energy (26). The training problem is then stated as a mean-field optimal control problem to determine the stopping time T , or time discretisation after time normalisation, as

well as the network parameters. The continuous formulation as gradient flows allows for the subsequent analysis of stability. We refer to the original papers for detail [90, 91].

7 Learned primal-dual architectures

The previous learned gradient architectures can be extended by also including neural operators in the data space Y . The resulting learned iterative network does not fall into the larger classification of a learned gradient network and thus forms its own class. These *primal-dual* neural operator architectures, which are also called dual domain architectures [101], were first introduced in [5].

A learned primal-dual architecture is, as the name suggests, obtained by unrolling a suitable primal-dual proximal splitting scheme. Splitting schemes are designed to minimise convex objectives that are given as a sum of a differentiable functional and a possibly non-smooth functional. Primal-dual schemes were introduced to exploit structure in a wider range of minimisation problems than those handled by splitting methods and involve setting up two iterative schemes for explicitly updating the primal and the dual variable.

Such primal-dual proximal splitting schemes are particularly well suited to account for specific structure in minimising objectives that typically arise in variational regularisation of ill-posed inverse problems. The objective is given as a functional of the form in (26), i.e.

$$\mathcal{E}_g(f) := \mathcal{S}(f) + \mathcal{G}_g(\mathcal{A}f) \quad (39)$$

where $\mathcal{G}_g: Y \rightarrow \mathbb{R}$ is given as $\mathcal{G}_g(h) := \mathcal{L}_Y(h, g)$, so $\mathcal{G}_g(\mathcal{A}f) = \mathcal{Q}_g(f)$ in the earlier notation. The primal variable in a primal-dual scheme will then represent the signal in X -space, and the dual variable (in the Hilbert space setting) can be identified with the data variable in Y -space.

An early example of a primal-dual proximal splitting scheme is the Arrow-Hurwicz algorithm [18]. When used for minimising $\mathcal{E}_g(f)$ in (39), it takes the form

$$\begin{cases} g^{k+1} := \text{prox}_{\sigma \mathcal{G}_g^\#}(g^k + \sigma \mathcal{A}f^k) \\ f^{k+1} := \text{prox}_{\sigma \mathcal{S}}(f^k - \sigma \mathcal{A}^*g^{k+1}) \end{cases} \quad \text{for } k = 0, 1, 2, \dots \quad (40)$$

Here, the step length $\sigma > 0$ is chosen appropriately to ensure convergence and $\mathcal{G}_g^\#: Y \rightarrow \mathbb{R}$ is the convex conjugate (Fenchel conjugate) of \mathcal{G}_g , which in the Hilbert space setting can be defined as

$$\mathcal{G}_g^\#(h) = \sup_{h' \in Y} \langle h', h \rangle_Y - \mathcal{G}_g(h') \quad \text{for } h \in Y.$$

The primal-dual hybrid gradient algorithm [40] introduces the possibility to have separate step lengths for the primal and dual variables $\tau, \sigma > 0$. It also includes a momentum governed by $0 < \rho < 1$ in the update of the primal variable to accelerate the convergence rate, thus resulting in an iterative scheme of the following form:

$$\begin{cases} g^{k+1} := \text{prox}_{\sigma \mathcal{G}_g^\#}(g^k + \sigma \mathcal{A}\bar{f}^k) \\ f^{k+1} := \text{prox}_{\tau \mathcal{S}}(f^k - \tau \mathcal{A}^*g^{k+1}) \\ \bar{f}^{k+1} := f^{k+1} + \rho(f^{k+1} - f^k) \end{cases} \quad \text{for } k = 0, 1, 2, \dots \quad (41)$$

The convergence speed and versatility of such schemes has made them a popular choice for non-smooth minimisation that typically arises in variational regularisation of inverse problems.

A primal-dual type of iterative scheme, like (40) or (41), can serve as a blueprint for a learned iterative network architecture via unrolling. One could replace only the proximal related to the regulariser $\mathcal{S}: X \rightarrow \mathbb{R}$ in (39) with a neural operator, or both proximal operator with neural operators. The learned primal-dual architecture presented in [5] adopts the latter by unrolling the iterative scheme in (41) and replacing the proximal operators in both X - and Y -space with neural operators. This gives rise to the following learned reconstruction operator for $\mathcal{R}_\theta: Y \rightarrow X$ with $\theta := (\theta_0, \vartheta_0 \dots, \theta_{N-1}, \vartheta_{N-1})$ where $\mathcal{R}_\theta(g) = f^N$ is given as

$$\begin{cases} g^{k+1} := \Gamma_{\vartheta_k}(g^k, \mathcal{A} f^k, g) \\ f^{k+1} := \Lambda_{\theta_k}(f^k, \mathcal{A}^* g^{k+1}) \end{cases} \quad \text{for } k = 0, 1, \dots, N-1. \quad (42)$$

In the above, we assume there is an initialisation $(f^0, g^0) \in X \times Y$, typically chosen as $g^0 := g$ and $f^0 := \mathcal{R}_0(g)$ as initial reconstruction from a handcrafted reconstruction operator. The two neural updating operators $\Lambda_{\theta_k}: X \times X \rightarrow X$ and $\Gamma_{\vartheta_k}: Y \times Y \times Y \rightarrow Y$ replace the proximal operators in (40). We note, that similar architectural choices as for learned gradient networks are possible, such as weight-sharing, memory for primal and dual variables space, as well as residual formulations of the update.

The use of the two spaces and associated neural updating operators instead of one improves expressivity of the learned reconstruction operator due two primary factors. First, and most obvious, the use of two neural operators doubles the number of learnable parameters and hence provides a stronger approximation capacity. Second, the added information in the dual space encodes crucial information on topology of the data and enables direct suppression of noise.

Remark 7.1. *Learned primal-dual architectures in (42) extend the learned gradient scheme in (17). To see this, note that setting $\Gamma_{\vartheta_k}(h, h', h'') = h' - h''$ (independent of h) in (42) yields the learned least squares architecture in (22).*

To summarise, learned primal-dual architectures extend learned gradient networks by introducing a second neural updating operator in the data space. This allows to increase expressivity for a fixed amount of iterations, and hence under the same associated cost with evaluating the forward \mathcal{A} and adjoint \mathcal{A}^* operator.

Implementation The original implementation in [5] is largely similar to the implementation of the learned least squares network [6] as described in Section 6.1.1. Specifically, both neural updating operator $\Lambda_{\theta_k}: X \times X \rightarrow X$ and $\Gamma_{\vartheta_k}: Y \times Y \times Y \rightarrow Y$ are parametrised as a ResNet style CNN. Additionally, a memory in both primal and dual variable has been used.

As before, the resulting learned reconstruction operator can be trained depending on available data and possible loss functions. Even though supervised and end-to-end training is the most successful, some studies have utilised unsupervised data [112, 131]. One should note, that the greedy training in (25) does not easily generalise to primal-dual algorithms. A greedy training objective for

the primal variable in image space X is straight-forward to establish, but the optimal loss for the data space Y is not well defined neither available and hence it remains an open problem, if greedy training is possible and in particular useful for primal-dual architectures.

8 Non-linear inverse problems and higher order methods

The previous section have been concentrated on learned reconstruction operators with linear forward operators, in the following we will now consider the more general setting where the forward operator $\mathcal{A}: X \rightarrow Y$ in the inverse problem (2) may be non-linear and is assumed to be Fréchet differentiable. To simplify the setting somewhat, we will still restrict our attention to the case when X and Y are Hilbert spaces. In fact, we will first see that the previous two sections on gradient networks and primal dual networks can be readily extended to the nonlinear case.

8.1 Learned gradient networks for non-linear problems

Since \mathcal{A} is assumed to be Fréchet differentiable, we get that the functional $\mathcal{Q}_g: X \rightarrow \mathbb{R}$ with $\mathcal{Q}_g(f) = \frac{1}{2} \|\mathcal{A}(f) - g\|_Y^2$ as in (15) is also Fréchet differentiable and its derivative is a bounded linear operator $\partial \mathcal{Q}_g(f): X \rightarrow X$. Next, X is a Hilbert space so from Riesz representation theorem we know there exists a unique element $\nabla \mathcal{Q}_g(f) \in X$, the gradient of \mathcal{Q}_g , such that

$$\partial \mathcal{Q}_g(f)(u) = \langle \nabla \mathcal{Q}_g(f), u \rangle_X \quad \text{for all } u \in X.$$

One can now use a gradient descent scheme as in (14) to compute a minimiser to the functional $\mathcal{Q}_g: X \rightarrow \mathbb{R}$. This yields an iterative scheme of the form

$$f^{k+1} = f^k - \beta_k \Delta f^k \quad \text{where } \Delta f^k := \nabla \mathcal{Q}_g(f^k).$$

A particular case of interest is when \mathcal{Q}_g is given as in (15). Then

$$\nabla \mathcal{Q}_g(f) = [\partial \mathcal{A}(f)]^* (\mathcal{A}(f) - g) \quad \text{for } f \in X \tag{43}$$

where the linear mapping $[\partial \mathcal{A}(f)]^*: Y \rightarrow X$ is the adjoint of the derivative of the forward operator at $f \in X$. The above iterative scheme becomes

$$f^{k+1} = f^k - \beta_k [\partial \mathcal{A}(f^k)]^* (\mathcal{A}(f^k) - g).$$

Unrolling the above scheme in the same way as in section 6 yields a learned operator architecture for solving ill-posed non-linear inverse problems. Analogous, we can replace the linear forward operator for the primal-dual schemes in Section 7 with the nonlinear forward $\mathcal{A}: X \rightarrow Y$ and the adjoint with the adjoint of its derivative $[\partial \mathcal{A}(f)]^*: Y \rightarrow X$ to obtain a learned-primal dual architecture for nonlinear inverse problems.

8.2 Newton and Newton-type methods

For nonlinear inverse problems the computation of the Fréchet derivative is usually computationally more demanding, as it depends on the current solution and needs to be re-computed every time. Thus, optimisation algorithms with faster convergence rates are often preferred to gradient-based and first order methods. Therefore, we will now discuss Newton methods and Newton-type methods as well as the corresponding learned reconstruction operators that result from unrolling them.

8.2.1 Newton iterates

When computing least-squares solutions to the inverse problem in (2) with X, Y Hilbert spaces, the solution is a minimiser to $\mathcal{Q}_g: X \rightarrow \mathbb{R}$ in (15). Therefore, also a critical point to \mathcal{Q}_g and a natural approach for computing it is based on solving $\nabla \mathcal{Q}_g(f) = 0$ in X . If \mathcal{Q}_g is twice Fréchet differentiable, then it is natural to consider (relaxed) Newton iterates for computing a minimiser by solving $\nabla \mathcal{Q}_g(f) = 0$. These yield a sequence $(f^k)_k \subset X$ generated by an iterative scheme of the form

$$f^{k+1} = f^k + \omega_k \Delta f^k \quad \text{where} \quad \Delta f^k := -[\text{Hess}(\mathcal{Q}_g)(f^k)]^{-1}(\nabla \mathcal{Q}_g(f^k)). \quad (44)$$

Here, $\text{Hess}(\mathcal{Q}_g): X \rightarrow \mathcal{L}(X, X)$ is the Hessian of \mathcal{Q}_g (Section A.2) and the step-length $0 < \omega_k \leq 1$ is chosen to ensure the objective function \mathcal{Q}_g decreases 'sufficiently' much along the Newton direction Δf^k . The corresponding reconstruction operator $\mathcal{R}: Y \rightarrow X$ is then given by $\mathcal{R}_\theta(g) := f^N$ with

$$\begin{cases} f^0 := \mathcal{R}_0(g) \\ f^k := f^{k-1} + \omega_k \Delta f^{k-1} \quad \text{for } k = 1, \dots \end{cases} \quad (45)$$

Computing the Newton direction Δf^k requires inverting the Hessian operator of \mathcal{Q}_g at each iterate f^k and this quickly becomes computationally unfeasible. If the main computational bottle neck lies in the inversion, then one could consider computing the Newton direction by solving the linear system

$$[\text{Hess}(\mathcal{Q}_g)(f^k)](\Delta f^k) = -\nabla \mathcal{E}(f^k)$$

When the Hessian is a positive definite operator, then one can consider various iterative approaches for solving the above linear problem. However, the mere task of forming the Hessian is often computationally unfeasible in its own right. Much effort has therefore been devoted to formulating various computationally feasible approximations to the Hessian or its inverse. We will consider next two of these, namely Gauss-Newton methods (Section 8.2.2) and quasi-Newton methods (Section 8.2.3), which basically provide a different update direction Δf for the reconstruction operator (45).

8.2.2 Gauss-Newton methods

The starting point is to consider Newton iterates (44) for computing a least squares solution to the inverse problem in (2). This requires computing the inverse of the Hessian of \mathcal{Q}_g in (15) at each iterate. Due to the aforementioned

cost of computing the Hessian $\text{Hess}(\mathcal{Q}_g)(f^k) \in \mathcal{L}(X, X)$ given in (67) the idea is now to approximate it by dropping the 2nd term, so that we get

$$\text{Hess}(\mathcal{Q}_g)(f^k) \approx [\partial\mathcal{A}(f^k)]^* \circ \partial\mathcal{A}(f^k).$$

This resulting scheme is $f^{k+1} = f^k + \omega_k \Delta f^k$ where

$$\Delta f^k := \left([\partial\mathcal{A}(f^k)]^* \circ \partial\mathcal{A}(f^k) \right)^{-1} (\nabla \mathcal{Q}_g(f^k)). \quad (46)$$

Computing the Hessian (or its inverse) can however be ill-conditioned, and this is especially the case for ill-posed inverse problems. Thus, one may consider applying the above iterative scheme not on $\mathcal{Q}_g: X \rightarrow \mathbb{R}$, but on a regularised version $\mathcal{E}_g: X \rightarrow \mathbb{R}$ of the form

$$\mathcal{E}_g(f) := \mathcal{Q}_g(f) + \alpha \mathcal{S}(f, u)$$

where $\mathcal{S}(\cdot, u): X \rightarrow \mathbb{R}$ for given $u \in X$ is assumed to be twice Fréchet differentiable with Hessian $\text{Hess}(\mathcal{S}(\cdot, u)): X \rightarrow \mathcal{L}(X, X)$. This leads to the following Gauss-Newton type of scheme where the Newton direction $\Delta f^k \in X$ in (46) is replaced with

$$\Delta f^k := \left([\partial\mathcal{A}(f^k)]^* \circ \partial\mathcal{A}(f^k) + \text{Hess}(\mathcal{S}(\cdot, f^{k-1}))(f^k) \right)^{-1} (\nabla \mathcal{E}_g(f^k)). \quad (47)$$

This was first introduced in [24] for regulariser $\mathcal{S}(f, u) = \|f - u\|^2$ (classical Tikhonov functional). An alternative popular choice for $\mathcal{S}: X \rightarrow \mathbb{R}$ is given by smoothed total variation [60] to ensure twice differentiability.

Learned Gauss-Newton Unrolling the iterative scheme in (45) where Δf^k is given as in (46) or (47) yields the *learned Gauss-Newton* neural operator for solving the inverse problem in (2). More precisely, this is a learned reconstruction operator $\mathcal{R}_\theta: Y \rightarrow X$ with $\theta := (\theta_1, \dots, \theta_N)$ that is given as $\mathcal{R}_\theta(g) := f^N$ where

$$\begin{cases} f^0 := \mathcal{R}_0(g) \\ f^k := \Lambda_{\theta_k}^k(f^0, \Delta f^0, f^1, \Delta f^1, \dots, f^{k-1}, \Delta f^{k-1}) \quad \text{for } k = 1, \dots, N. \end{cases} \quad (48)$$

where $\Lambda_{\theta_k}^k: (X \times X)^k \rightarrow X$ are neural operators with suitable architectures. The weights θ_k are learned during training whereas the Newton directions $\Delta f^k \in X$ are handcrafted as in (46) or (47).

A special case considered by [76, 111] is (48) without memory and $\mathcal{S}: X \rightarrow \mathbb{R}$ set to a Gaussian with co-variance operator $\Sigma_S: X \rightarrow X$, i.e.,

$$\mathcal{S}(f) = \exp\left(-\frac{1}{2}\langle \Sigma_S(f), f \rangle\right)$$

where $\Sigma_S: X \rightarrow X$ is bounded, self-adjoint and non-negative. Then (48) becomes

$$f^{k+1} := \Lambda_{\theta_k}\left(f^k, \left([\partial\mathcal{A}(f^k)]^* \circ \partial\mathcal{A}(f^k) + \Sigma_S\right)^{-1} (\nabla \mathcal{E}_g(f^k))\right) \text{ for } k = 1, \dots, N$$

where $\Lambda_{\theta_k}: X \times X \rightarrow X$ is a neural operator with suitable architecture. The training in [76, 111] has been done following the greedy regime (25). Whereas the an end-to-end training of the learned reconstruction operator has been utilised in [47, 108].

8.2.3 Quasi-Newton methods

The approach here is to iteratively approximate the Hessian or its inverse in (44). This results in the following scheme: $f^{k+1} = f^k + \omega_k \Delta f^k$ where

$$\Delta f^k := \begin{cases} \mathcal{H}_k^{-1}(\nabla \mathcal{Q}_g(f^k)) & \text{with } \mathcal{H}_k \approx \text{Hess}(\mathcal{Q}_g)(f^k) \\ \mathcal{B}_k(\nabla \mathcal{Q}_g(f^k)) & \text{with } \mathcal{B}_k \approx [\text{Hess}(\mathcal{Q}_g)(f^k)]^{-1}. \end{cases} \quad (49)$$

The approximations $\mathcal{B}_k, \mathcal{H}_k: X \rightarrow X$ typically need to satisfy a secant condition:

$$\begin{aligned} \nabla \mathcal{Q}_g(f^{k+1}) &= \nabla \mathcal{Q}_g(f^k) + \mathcal{H}_k(f^{k+1} - f^k) \\ f^{k+1} - f^k &= \mathcal{B}_k(\nabla \mathcal{Q}_g(f^{k+1}) - \nabla \mathcal{Q}_g(f^k)). \end{aligned} \quad (50)$$

Various methods have been developed for constructing \mathcal{H}_k or \mathcal{B}_k when $X = \mathbb{R}^n$. In that setting, $\mathcal{Q}_g: \mathbb{R}^n \rightarrow \mathbb{R}$ so its Hessian is represented by a symmetric $n \times n$ matrix. The symmetric linear operators $\mathcal{B}_k, \mathcal{H}_k: \mathbb{R}^n \rightarrow \mathbb{R}^n$ are therefore represented by $n \times n$ matrices \mathcal{B}_k and \mathcal{H}_k , respectively. Quasi-Newton methods now provide explicit closed-form expressions for assembling \mathcal{B}_k and \mathcal{H}_k from previous iterates that only make use of first order information. Examples include the Davidon-Fletcher-Powell (DFP), Broyden-Fletcher-Goldfarb-Shanno (BFGS), symmetric rank-one (SR1) and Powell-Symmetric-Broyden (PSB) methods that are nowadays widely used in non-linear programming. As an illustration, we provide the expressions used within the widely used BFGS scheme:

$$\begin{aligned} \mathcal{H}_{k+1} &= (\mathbf{I} - \gamma_k(\delta f_k \cdot \delta \mathcal{Q}_k^\top)) \cdot \mathcal{H}_k \cdot (\mathbf{I} - \gamma_k(\delta \mathcal{Q}_k \cdot \delta f_k^\top)) + \gamma_k(\delta f_k \cdot \delta f_k^\top) \\ \mathcal{B}_{k+1} &= \mathcal{B}_k - \frac{1}{\langle \delta f_k, \mathcal{B}_k \cdot \delta f_k \rangle} ((\mathcal{B}_k \cdot \delta f_k) \cdot (\delta f_k^\top \cdot \mathcal{B}_k)) + \gamma_k(\delta \mathcal{Q}_k \cdot \delta \mathcal{Q}_k^\top) \end{aligned} \quad (51)$$

where $\delta f_k := f^{k+1} - f^k$, $\delta \mathcal{Q}_k := \nabla \mathcal{Q}_g(f^{k+1}) - \nabla \mathcal{Q}_g(f^k)$, and $\gamma_k := 1/\langle \delta f_k, \delta \mathcal{Q}_k \rangle$.

Last two decades has seen efforts in extending quasi-Newton schemes of the above type to the infinite-dimensional Hilbert space setting. These are nicely summarised in [143] that provides Hilbert space versions of the BFGS, DFP, SR1, and PSB schemes. The derivations are based on the observation that a quasi-Newton update formula along with the secant condition can be expressed as a solution to a specific constrained variational problem over the space of symmetric matrices. Formulating and solving the corresponding variational problem over the space of bounded symmetric operators in Hilbert spaces (see [143, Corollary 3.3]) yields the functional analytic version of the quasi-Newton update formula. The generalisation of the BFGS scheme in (51) to the functional analytic setting reads as follows:

$$\begin{aligned} \mathcal{H}_{k+1} &= (\mathcal{I} - \gamma_k(\delta f_k \otimes \delta \mathcal{Q}_k)) \circ \mathcal{H}_k \circ (\mathcal{I} - \gamma_k(\delta f_k \otimes \delta \mathcal{Q}_k)) + \gamma_k(\delta f_k \otimes \delta f_k) \\ \mathcal{B}_{k+1} &= \mathcal{B}_k - \frac{1}{\langle \delta f_k, \mathcal{B}_k(\delta f_k) \rangle} (\mathcal{B}_k(\delta f_k) \otimes \mathcal{B}_k(\delta f_k)) + \gamma_k(\delta \mathcal{Q}_k \otimes \delta \mathcal{Q}_k) \end{aligned} \quad (52)$$

where $\delta f_k, \delta \mathcal{Q}_k$ and γ_k are defined as in (51) and the \otimes -operator is defined as follows: $f \otimes u: X \rightarrow X$ for given $f, u \in X$ is the linear rank one operator $v \mapsto \langle u, v \rangle f$. On a final note, one can show that if the curvature condition $\langle \delta f_k, \delta \mathcal{Q}_k \rangle > 0$ holds, then $\mathcal{B}_k, \mathcal{H}_k \in \mathcal{L}(X, X)$ in (52) are self-adjoint, invertible, and positive definite.

Learned quasi-Newton Similar to how learned Gauss-Newton architectures were defined by unrolling a Gauss-Newton scheme (Section 8.2.2), we can also define learned quasi-Newton architectures by unrolling a quasi-Newton scheme that has the form (49).

This yields a learned reconstruction operator $\mathcal{R}_\theta: Y \rightarrow X$ with $\theta := (\theta_1, \dots, \theta_N)$ that is given as in Learned Gauss-Newton (48), but this time with Newton directions $\Delta f^k \in X$ that are handcrafted as in (49). One has in addition the possibility to enforce the secant conditions in (50). This could be achieved either by introducing additional terms to the loss during training of \mathcal{R}_θ . One could in addition also modifying the architecture to ensure that it satisfies hard constraints of the above type without sacrificing model capacity [109]. Examples of learned quasi-Newton schemes in the literature are considered in [108] for SR1 updates and in [136] based in Broyden’s method.

8.2.4 Additional notes and remarks

Based on the reconstruction operator in (45) one could construct a large class of learned reconstruction operators by replacing the Newton directions u with suitable choices. One may even consider learned directions instead of handcrafted update directions.

Additionally, one can also construct neural operator architectures by unrolling proximal Newton and proximal quasi-Newton schemes and then replacing the proximal with a neural operator are possible. This approach was considered in the learned proximal regularised Gauss-Newton network [10], see also [47].

Another computational challenge exists due to the fact that many nonlinear inverse problems are given by a PDE that is solved with finite element methods (FEM). That means, the reconstructions and iterates f^k are given on usually triangular FE meshes and hence a neural update operator Λ_θ based on CNNs is not directly applicable. This can be overcome for instance by interpolation to a rectangular pixel mesh [111] or by using rectangular meshes [108] to begin with. Alternatively, some authors [10, 76] have utilised graph neural networks to operate on FE meshes. This is a natural choice, where the adjacency matrix in the graph neural network encodes the neighbouring elements and hence allows for computation over irregular meshes. This has been realised as a promising and flexible alternative to train a learned reconstruction operator that is mesh and dimension agnostic [75, 141].

9 Implementation related aspects

9.1 Performance and interpretability

The performance of a learned reconstruction method for solving an ill-posed inverse problem will depend on a number of choices. The first choice relates to which neural operator architecture one will use. This is the main topic of the chapter and it affects the accuracy and robustness of the learned reconstruction method. As outlined in Section 5.2, the architecture needs to incorporate some level of domain adaptation as in learned iterative networks that are especially well suited to approximate operators which are defined implicitly through an iterative scheme. This typically covers operators that regularise ill-posed inverse problems (Section 2.1) but also optimisation solvers (Section 2.2).

The next choice relates to setting up the learning problem. The various options are briefly discussed in Section 4 and it is here important to setup a learning problem that is consistent with the type of training data one has. The choice of loss function used in training will in particular determine what statistical estimator the learned reconstruction method approximates. Hence, in contrast to what is claimed in [110], using an unrolled architecture as in learned iterative networks does not in itself improve upon interpretability. As an example, if one uses a loss that is the squared 2-norm, then a perfectly trained learned operator will approximate the conditional expectation. Likewise, using the 1-norm as loss implies that the operator learning approximates the conditional median. The choice of architecture is more related to how good this approximation becomes for some given set of training data.

To summarise, the choice of loss function along with type of training data dictates *what* one seeks to compute. The Choice of neural operator architecture is more related to *how to compute* as it influences the model capacity and generalisation gap. We refer to the surveys [70, 84, 113] for further discussions on interpretability and theoretical results for learned reconstructions.

9.2 Hyper-parameter tuning

Besides choices of architecture and learning problem (incl. choice of loss function), it is also well-known that the performance of a neural network depends on hyper-parameter settings [34, 120, 148, 146, 122]. These hyper-parameters typically regulate the optimisation method used during the training.

Section C provides a very brief introduction to gradient descent schemes that are commonly used for training deep neural networks. Typical hyper parameters that are varied during the training are the learning rate, choice of batch size n_k (minibatches are typically selected as random subsets of the training data), and initialisation. Empirical experience indicates that it is often enough to use default settings of these hyper-parameters in training many learned iterative networks.

There is, however, no methodology in place for tuning a hyper-parameter if that need rises apart from trial-and-error. For example, with respect to neural network size, it is common to start with a ResNet type architecture as updating operator in the learned reconstruction operator [5, 6]. In case, performance is not satisfactory, one may increase expressivity of the updating operator by either adding more convolutional layers or use a more expressive architecture like a U-Net for the updating operator [72]. Usually, one will observe a plateau in performance while increasing expressivity of the neural network, indicating a somewhat optimised choice.

9.3 Risk of overfitting

An advantage that learned iterative networks have over domain agnostic neural network architectures is that the former has much fewer learnable parameters (Section 5.2). This reduces the risk for overfitting. Since training data is finite, empirical risk minimization will lead to overfitting, e.g., the optimal parameter computed from training data will differ to one computed from all possible training data, and parameters that minimise the empirical risk will not be optimal for the expected risk.

Classical statistical learning theory dictates that more parameters increases the risk of overfitting, although this has recently been called into question [46, 95, 132]. Learned iterative networks have advantageous properties over domain agnostic architectures since the number of learnable parameters is typically much smaller. In particular, this should also be taken into account when optimising the network architecture for performance as outlined above and hence out-of-distribution tests are necessary to properly judge performance.

9.4 Complexity of implementation

A specific challenge that arises when training a learned iterative network is to ensure the software libraries used for computing the handcrafted components are seamlessly integrated with the deep learning framework used for setting up and training the neural network. This means in particular that it must be possible to cast these handcrafted components as layers within the architecture for the learned iterative network. In addition, one must also ensure the chain rule works as expected when the network is differentiated with automatic differentiation.

Deep neural networks are typically trained with gradient methods that (approximately) compute a (local) minimiser to a highly non-linear and non-convex objective, see Appendix C. This objective takes a large number of neural network parameters as input, so a gradient scheme typically involves computing gradients in a high dimensional space. One therefore uses automatic differentiation (by reverse mode) for this purpose, see Appendix B and [32] for more details. Here we simply note that usage of automatic differentiation has been greatly simplified [29] thanks to well-maintained and highly optimised libraries that form the backbone of contemporary deep learning, like TensorFlow [3] or PyTorch [119]. These allow for computing gradients of standard neural network components, but they very rarely implement a simulator, e.g., the implementation of a forward operator in inverse problems. Hence, setting up and training a learned iterative network that incorporate a simulator would require one to seamlessly integrate external domain specific software components for the simulator (and the adjoint of its derivative) with frameworks for differentiable programming. An option is to re-implement the simulator within a framework that supports differentiable programming, like JAX [37, 100] or DiffTaichi [77]. Examples of such differentiable simulators are [116] for rigid-body simulation, [83, 153] for rendering of complex light transport effects, and Mitsuba 3 [81] for Monte Carlo based simulation of forward and inverse light transport.

However, rewriting highly optimised software libraries for specific simulators is often unpractical. This is especially the case when the library in question is extensive and highly optimised, like ASTRA [1, 2] for simulating tomographic imaging with various acquisition geometries and FEniCS/Dolphin [11, 103, 104] for finite element based simulation of systems modelled by (coupled) PDEs. A far more pragmatic approach is to use the external libraries unaltered. Which requires one to either manually define the automatic differentiation rules within the learning libraries or a more streamlined approach is possible if one wraps the operators defined through the external libraries using some binding library, like ODL [6] or DeepInverse [138].

In summary, the implementation of learned iterative methods involves another layer of computational complexity and hence often requires further domain knowledge. Consequently, it is not as accessible as an out-of-the-box neural net-

work for image processing. This underlines the importance of open access codes accompanying papers which present new learned iterative methods as well as the development of designated software packages for learned reconstructions.

9.5 Computational feasibility of training

Computational feasibility of the training is a major challenge in using learned iterative networks as already discussed in Section 6.1.1. Let us recall, that in the supervised training as outlined in Section 4.1 one would like to train \mathcal{R}_θ end-to-end given supervised training data $(f_i, g_i) \in X \times Y$ by minimising

$$\hat{\theta} = \arg \min_{\theta \in \Theta} \sum_i \mathcal{L}_X(\mathcal{R}_\theta(g_i), f_i).$$

Nevertheless, this requires evaluation of the forward operator \mathcal{A} and the adjoint of its derivative (\mathcal{A}^* if it is linear) in each forward as well as backward pass N -times for each training iterations, which will be well in ten thousands. This can quickly become computationally unfeasible as training can involve many epochs, and especially so in 3D imaging problems or nonlinear inverse problems where the Fréchet derivates, or Jacobians in the discrete setting, need to be recomputed for each unrolled as well as training iteration.

This training problem has been tackled by uncoupling training of the network components and evaluation of the operators, or the iterative schemes, as discussed earlier by reformulating the end-to-end training into a greedy approach (25) as done in [9, 73] for large scale linear inverse problems and in [76, 111] for nonlinear inverse problems. Another popular option is given by plug-and-play approaches as discussed in Section 6.1.2, here the updating network is trained as a denoiser independent of the iterative scheme, see [84] for a survey.

Alternatively, one can aim to reduce the computational cost of the operator itself to enable feasible training times as well as faster inference. Clearly, one could learn the operator itself [16, 63, 137]. Nevertheless, conceptually this amounts to introducing another learned component in the network and will remove the handcrafted nature of the domain adaptation, especially if generic neural operators are used. Another option to reduce the computational cost of the forward operator include approximations [71, 72, 106, 137], model-reductions or discretisations [68], as well as optimised numerical implementations for special cases [62, 69].

On a final note, one may also consider using gradient checkpointing during training. This significantly reduces the memory footprint during backpropagation that can easily become prohibitively large for a learned iterative network. However, GPU computation is delayed/paused during checkpoint saving for checkpoint GPU-CPU transfer, resulting in significant training interruptions and reduced training throughput. One can to some extent mitigate this slow down in training by considering other checkpointing strategies [152].

10 Numerical examples for choice of update directions

We will conclude this chapter with a numerical study on performance differences for various formulations of the reconstruction operator. One goal is to

understand to what extend the different formulations in result in performance differences. Naturally, a comprehensive study on all choices is out of scope, but we aim to give a intuition here on the influence of such design choices.

In the first part we will examine the discussed unrolling schemes for linear inverse problems under largely same training schemes. In the second part we will shortly present recent results for nonlinear inverse problems and the influence of update directions for the learned reconstruction, together with a comparison of greedy vs. end-to-end training relevant for expensive nonlinear problems.

10.1 Comparison for linear problem

We consider a standard reconstruction problem in sparse view and low-dose CT imaging in fan-beam geometry in two dimensions. The forward operator is given by the X-ray transform

$$\mathcal{A}f = \int_{L(\varphi, r)} f(s)ds = g,$$

where the integration is over lines $L(\varphi, r)$ parametrised by an angle $\varphi \in [0, 2\pi)$ and location on the detector $r \in \mathbb{R}$. The geometry for each line is then defined by measurement specific variables describing distances between source, object, and detector. The forward operator is implemented using the Astra toolbox [1] supporting GPU computations.

For this study we chose 120 equidistant angles, 256 detection points on the detector, i.e., 256 lines per angle, and 2% relative Gaussian noise. The target images are of resolution 128×128 . We sample training data from a distribution of up to 50 random ellipses in the image and create a test set of fixed 50 samples for evaluating the performance after training. The loss functions are chosen to be fully supervised

$$\hat{\theta} = \arg \min_{\theta \in \Theta} \sum_i \mathcal{L}_X(\mathcal{R}_\theta(g_i), f_i),$$

with training samples drawn from randomly generated ellipses sampled new for each training iteration. An illustration of a ground-truth image f_i , obtained noisy measurement g_i , and initial reconstruction by filtered backprojection $f_i^0 = \mathcal{R}(g_i)$ are shown in Figure 1.

We will consider the previously presented options for learned reconstruction operators $\mathcal{R}_\theta: Y \rightarrow X$ for the linear inverse problem. That is, the three classes for learned gradient networks, namely learned least squares networks 6.1.1, proximal networks 6.1.2, and variational networks 6.1.3. That is we have the following update rules with $\nabla \mathcal{Q}_g(f) = \mathcal{A}^*(\mathcal{A}f - g)$ in respective order:

$$f^k := \Lambda_{\theta_k} \left(f^{k-1}, \nabla \mathcal{Q}_g(f^{k-1}) \right) \quad (53)$$

$$f^k := \Lambda_{\theta_k} \left(f^{k-1} - \omega \nabla \mathcal{Q}_g(f^{k-1}) \right) \quad (54)$$

$$f^k := f^{k-1} - \omega \nabla \mathcal{Q}(f^{k-1}, g) + \Lambda_{\theta_k}(f^{k-1}). \quad (55)$$

For the two last updates, we also learn the step-size parameter ω shared for all iterates. Additionally, we consider the learned primal dual as presented in

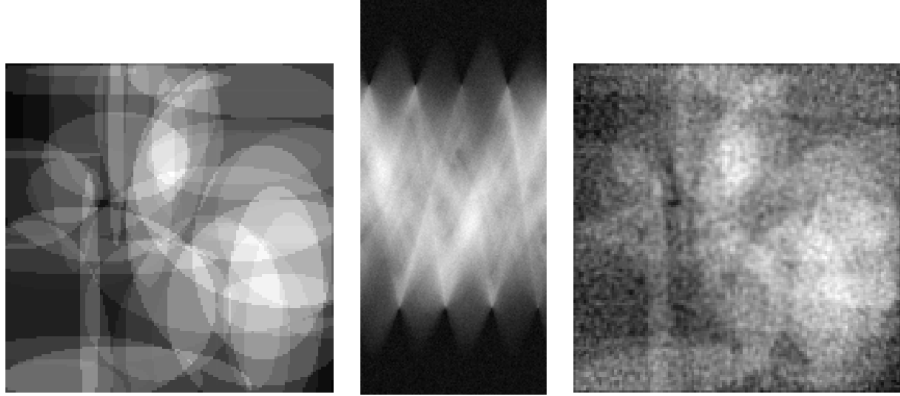


Figure 1: Illustration of measurement setup. (Left) ground-truth, (Middle) sinogram with 120 angles and 2% noise, (Right) Reconstruction via filtered backprojection.

Section 7 with two update networks:

$$\begin{cases} g^k := \Gamma_{\theta_k}(g^{k-1}, \mathcal{A} f^{k-1}, g) \\ f^k := \Lambda_{\theta_k}(f^{k-1}, \mathcal{A}^* g^k). \end{cases} \quad (56)$$

Each reconstruction operator starts with the initial reconstruction given by the filtered backprojection $f_i^0 = \mathcal{R}(g_i)$. The result of the learned reconstruction operator is then given by the final iterate $\mathcal{R}_\theta(g_i) = f_i^N$, depending on the corresponding update equation above. We have made an effort to choose the networks and parameter count largely the same, as well as training protocols. We note, that better results may be obtained if training protocols and parameter choices are optimised for each algorithm separately. Additionally, the implementation may differ from the original published versions. Nevertheless, the purpose here is to present a direct comparison under same environmental choices.

The subnetworks Λ_θ and Γ_θ for all approaches are chosen as ResNet [74] style with 5 convolutional layers in total, the first layer expands the input to 32 channels, followed by 3 layers with each 32 channels, and a final layer collapsing to one output channel. Each layer has 3×3 convolutional kernels, bias, and ReLU as nonlinearity, except the final layer, which does not employ a nonlinearity important for the update. All learned reconstruction operators are trained for 25000 iterations, with initial learning rate of 10^{-3} and cosine annealing. The performance is then evaluated at the end for the test ellipses. The results of the trained networks are summarised in Table 1.

We can see from the quantitative results that the reconstruction quality for all methods is rather close. Especially all learned gradient networks perform very similar, whereas LPD provided a small increase in performance with the same number of iterations. For the gradient networks it is interesting to observe that the performance increases with decreasing structure, that means the performance decreases, albeit only slightly, with more handcrafted components. In other words, the more freedom the network has to learn, the better it performs. It should be noted though that the test data is in distribution and

Table 1: Comparison of learned reconstruction operators based on different unrolling schemes. PSNR is reported as average over 50 test samples.

	VarNet	Proximal	Least Sq.	LPD	
Iterations	10	10	10	10	5
Parameter	283531	283531	286411	575710	287855
Training (min.)	48	48	49	56	35
PSNR (dB)	30.88	30.91	30.96	31.11	31.02

out-of-distribution generalisation may differ.

For LPD we see a clear improvement in performance, but under the same amount of iterations also the number of parameters doubles due to the two networks, one in data space Y and one in image space X . Thus, we have additionally performed a test with half the iterates, so that LPD has a similar parameter count as the gradient networks. Interestingly, LPD still provides the best reconstructions in terms of PSNR, but with a smaller improvement over the learned least squares network.

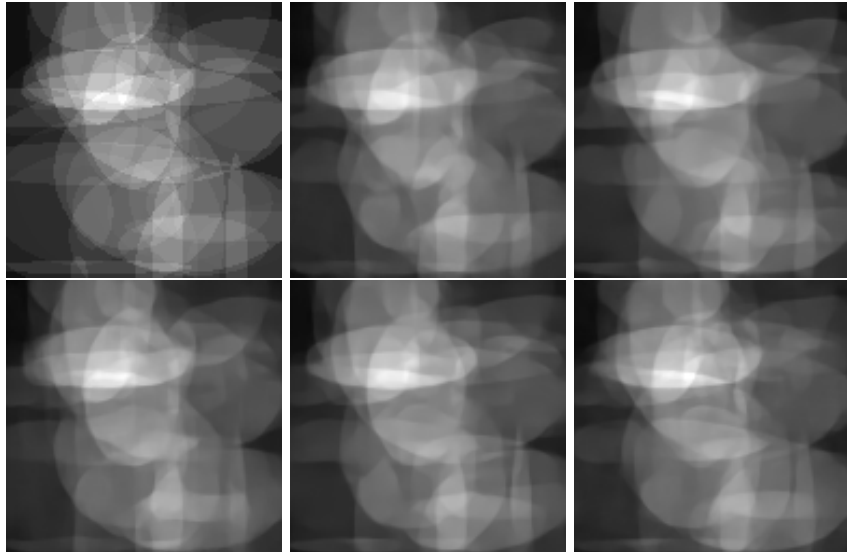


Figure 2: Comparison of reconstructions for the trained networks for one sample in the test data. From left to right and top to bottom: Ground truth, Variational Network, Proximal Network, Learned Least Squares, Learned Primal-Dual (5 iterates), Learned Primal-Dual (10 iterates).

Finally, we present the reconstructions obtained with each network in Figure 2. We can see that there is a clear difference in qualitative visual performance between the networks. The three gradient networks produce blurrier images, and LPD does provide a sharper reconstruction. The 10 iteration reconstruction with LPD is clearly the visually best performing, whereas the Variational Network result fails to recover many fine details. This is also reflected in the quantitative results.

10.2 Comparison for nonlinear problem

The research on unrolled methods for nonlinear inverse problems is much younger with few examples [10, 47, 76, 111, 108]. Where some approaches have considered a greedy training (25) to overcome the computational burden, as discussed in Section 6.1.1. Additionally, in the nonlinear case a large class of update directions is available to train the unrolled network. Hence, one major question is how the choice of update directions influence the performance of the learned reconstruction operator and how greedy training compared to end-to-end training influences the performance.

In the following we shortly present results from a recent study [108], which compares different update directions and training regimes for the nonlinear inverse problem of quantitative photoacoustic tomography (QPAT). For this purpose let us shortly discuss the basics of QPAT, where the goal is to recover the spatially distributed optical parameters of absorption μ_a and scattering μ_s by modelling the fluence Φ in biological tissue after illumination with a short laster pulse. The accurate model for light transport in this case is given by the radiative transfer equation, but to allow for efficient computations and training of the unrolled schemes the study [108] considers an elliptic approximation. That is, the underlying model equation in the domain Ω is then given by the diffusion approximation

$$-\nabla \cdot \kappa(r) \nabla \Phi(r) + \mu_a(r) \Phi(r) = q_0(r), \quad r \in \Omega, \quad (57)$$

where q_0 is the light source in Ω and the parameter $\kappa(r) = (n(\mu_a(r) + \mu'_s(r)))^{-1}$ in dimension $n = 2, 3$ is the diffusion coefficient where $\mu'_s = (1 - g)\mu_s$ is the reduced scattering coefficient with anisotropy parameter $-1 < g < 1$. Under suitable boundary conditions [14].

The inverse problem in QPAT is now to recover μ_a, μ_s in Ω from internal data. That is, the knowledge of the absorbed energy density $h \in \Omega$ given by

$$h = \mu_a \Phi(\mu_a, \mu_s), \quad (58)$$

where $\Phi(\mu_a(r), \mu_s(r))$ is the solution to the diffusion approximation (57). This internal data h can be obtained by solving the acoustic problem first, see [31] for a review.

The inverse problem (58) is usually solved by second order methods, such as Gauss-Newton and quasi-Newton methods. The paper [108] formulates a learned reconstruction operator to robustly recover the optical parameters considering that the diffusion approximation is not an accurate model. Additionally, it investigates how different choices for update directions and training schemes for the learned reconstruction operator in (48) effect the reconstruction quality. Specifically, the study compares choices learned gradient descent (Section 8.1), learned Gauss-Newton (Section 8.2.2), and learned quasi-Newton with an SR1 update (Section 8.2.3) for Δf . The learned reconstruction operator for all three cases is given by $\mathcal{R}_\theta(g) := f^N$ where

$$\begin{cases} f^0 := \mathcal{R}_0(g) \\ f^k := \Lambda_{\theta_k}(f^{k-1}, \Delta f^{k-1}) \quad \text{for } k = 1, \dots, N, \end{cases}$$

where $\Lambda_{\theta_k} : X \times X \rightarrow X$ uses a simple ResNet style architecture with 4 convolutional layers of 32 channels except the last one which contracts to the singular

output channel, similar to the linear inverse problem experiments above. Training is performed for both, end-to-end and greedy, given supervised training data with increasing amount of iterations. Additionally, a comparison to a simple U-Net post-processing is done as baseline.

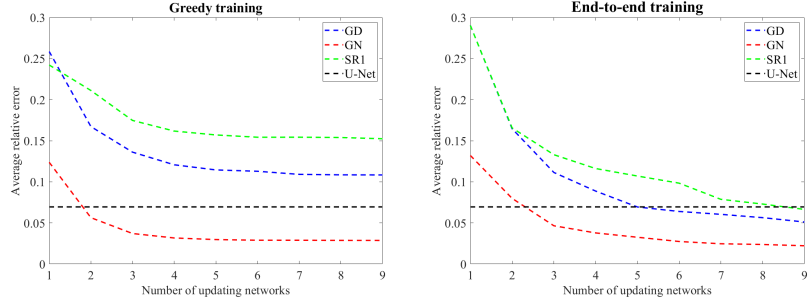


Figure 3: Comparison of training update directions and training schemes for learned reconstructions in QPAT. Shown is the relative error in reconstructed absorption coefficients μ_a for (Left) greedy training schemes and (Right) end-to-end, with three choices for the handcrafted update direction Δf as gradient descent (GD), Gauss-Newton (GN), and quasi-Newton SR1 update (SR1).

The results are presented in Figure 3 for the absorption coefficient μ_a only, where the scattering behaves. There are a few takeaways from the experiment. First, the learned Gauss-Newton performs well and largely similar for greedy and end-to-end training. Second, gradient descent and the quasi-Newton method does not perform satisfactory in greedy training. This is consistent with previous unreported experiments, that greedy training with gradient descent updates did not perform well for the study in [111]. Third, when trained end-to-end all algorithms are able to beat the U-Net baseline, but need larger amount of iterations. In conclusion this study indicates that learned Gauss-Newton clearly outperforms the other update directions and reinforces the use in previous papers. We refer to [108] for the experiments and an example for a digital twin introducing large modelling error that will be present in biological tissue.

11 Conclusions

This chapter aimed at developing a unified view on learned iterative reconstructions through the formulation of learned reconstruction operator. Specifically, we separated the *how to compute* via the learned reconstruction operator from the *what to compute* given by the learning problem. This independent treatment allows to identify structural similarities in many established approaches. In fact, we see in Section 6 that many approaches in the literature are the same in their core and only differ by a specific parametrisation of the neural updating operator. Furthermore, we have presented the framework of learned iterative reconstructions for the usual case of linear inverse problems as well as for nonlinear inverse problems in Section 8. Finally, the computational examples showed that for linear inverse problems and gradient networks, there is only minor difference between the different parametrisations. Whereas in nonlinear inverse

problems, the choice of update direction, or the underlying algorithm for the unrolled method, has a major effect on the performance.

We expect that this chapter will help researchers to view learned iterative reconstructions and learned reconstruction operators on a high level and will open new ideas to design suitable learned reconstructions for challenging inverse problems.

Acknowledgements

This work has been supported in parts by the Research council of Finland (Project No. 353093, Finnish Centre of Excellence in Inverse Modelling and Imaging; and Project No. 359186, Flagship of Advanced Mathematics for Sensing Imaging and Modelling; Projects No. 338408, Academy Research Fellow (AISOL); Project No. 370528, Academy project (AequiLoFi)) and in parts by the Swedish Research Council grants 2020-03107, Swedish Energy Agency P2022-00286, FORMAS 2022-00469. AH was supported by DigitalFutures Scholar-in-Residence grant KTH-RPROJ-0146472 2

A Common data loss functionals

Let Y be a (real) Hilbert space with inner product $\langle \cdot, \cdot \rangle_Y$ and associated norm $\|\cdot\|_Y$. A common special case for the data-fidelity $\mathcal{Q}_g: X \rightarrow \mathbb{R}$ in (13) is when the data loss is given as

$$\mathcal{L}_Y(g, h) := \mathcal{D}(g, h) \quad \text{for } g, h \in Y$$

where $\mathcal{D}: Y \rightarrow \mathbb{R}$ is some suitable functional. Then the data-fidelity is of the form

$$\mathcal{Q}_g(f) := \mathcal{D}(\mathcal{A}(f) - g) \quad \text{for } f \in X. \quad (59)$$

We next compute the gradient and the Hessian of such a data-fidelity functional.

A.1 Gradient calculations

When $\mathcal{A}: X \rightarrow Y$ is Fréchet differentiable, then one can derive an expression for the derivative and gradient of $\mathcal{Q}_g: X \rightarrow \mathbb{R}$ in (59). To see this, we first note that \mathcal{Q}_g is given by composing the mapping $\mathcal{A}(\cdot) - g$ with \mathcal{D} . Next, the derivative of $\mathcal{A}(\cdot) - g$ at $f \in X$ is the linear mapping $u \mapsto \partial\mathcal{A}(f)(u)$. Hence, by the chain rule we get that the derivative of \mathcal{Q}_g in (59) at $f \in X$ is the linear mapping $\partial\mathcal{Q}_g(f): X \rightarrow X$ given as

$$\partial\mathcal{Q}_g(f)(u) = \partial\mathcal{D}(\mathcal{A}(f) - g)(\partial\mathcal{A}(f)(u)) \quad \text{for } u \in X. \quad (60)$$

The associated gradient at $f \in X$ is the element $\nabla\mathcal{Q}_g(f) \in X$ that is given implicitly by the relation

$$\partial\mathcal{Q}_g(f)(u) = \langle \nabla\mathcal{Q}_g(f), u \rangle_X \quad \text{for any } u \in X. \quad (61)$$

The existence of a unique such element is guaranteed by the Riesz representation theorem. To get more explicit expressions for the derivative/gradient, we need to consider special cases of $\mathcal{D}: Y \rightarrow \mathbb{R}$ in (59).

$\mathcal{D}(g) := \|g\|_Y^2$: This choice corresponds to $\mathcal{Q}_g(f) = \|\mathcal{A}(f) - g\|_Y^2$ in (59). Next, $\partial\mathcal{D}(g)(h) = 2\langle g, h \rangle_Y$ for $g, h \in Y$. Inserting this into (60) yields

$$\begin{aligned} \partial\mathcal{Q}_g(f)(u) &= 2\langle \mathcal{A}(f) - g, \partial\mathcal{A}(f)(u) \rangle_Y \\ &= 2\langle (\partial\mathcal{A}(f))^*(\mathcal{A}(f) - g), u \rangle_Y. \end{aligned} \quad (62)$$

In the above, $\partial\mathcal{A}(f)^*: Y \rightarrow X$ is the linear mapping representing the adjoint of the derivative of $\mathcal{A}: X \rightarrow Y$ at $f \in X$ (think transpose of the Jacobian). Finally, comparing the rightmost expression in (62) with the equality in (61) yields

$$\nabla\mathcal{Q}_g(f) = 2(\partial\mathcal{A}(f))^*(\mathcal{A}(f) - g). \quad (63)$$

$\mathcal{D}(g) := \|g\|_Y$: This choice corresponds to $\mathcal{Q}_g(f) = \|\mathcal{A}(f) - g\|_Y$ in (59). Next, $\partial\mathcal{D}(g)(h) = \frac{1}{\mathcal{D}(g)}\langle g, h \rangle_Y$ for $g, h \in Y$. Inserting this into (60) yields

$$\begin{aligned} \partial\mathcal{Q}_g(f)(u) &= \frac{1}{\mathcal{D}(\mathcal{A}(f) - g)}\langle \mathcal{A}(f) - g, \partial\mathcal{A}(f)(u) \rangle_Y \\ &= \frac{1}{\|\mathcal{A}(f) - g\|_Y}\langle (\partial\mathcal{A}(f))^*(\mathcal{A}(f) - g), u \rangle_Y. \end{aligned} \quad (64)$$

Finally, comparing the rightmost expression in (64) with the equality in (61) yields

$$\nabla \mathcal{Q}_g(f) = \frac{1}{\|\mathcal{A}(f) - g\|_Y} (\partial \mathcal{A}(f))^* (\mathcal{A}(f) - g). \quad (65)$$

Note that the derivative/gradient of \mathcal{Q}_g at f only exists when $\mathcal{A}(f) - g \neq 0$. This is to be expected since \mathcal{D} is not differentiable at 0.

A.2 Hessian calculations

Assume now that $\mathcal{A}: X \rightarrow Y$ is twice Fréchet differentiable. Then \mathcal{Q}_g is also twice Fréchet differentiable. Its 2nd Fréchet derivative at $f \in X$ is a mapping $\partial^2 \mathcal{Q}_g(f): X \rightarrow \mathcal{L}(X, \mathbb{R})$ representing a symmetric bilinear form, i.e.,

$$(u, v) \mapsto \partial^2 \mathcal{Q}_g(f)(u)(v) \quad \text{is symmetric bilinear form.}$$

Analogous to the case with the first derivative, there exists a unique bounded linear operator $\text{Hess}(\mathcal{Q}_g): X \rightarrow \mathcal{L}(X, X)$ (Hessian of \mathcal{Q}_g) such that the following holds:

$$\partial^2 \mathcal{Q}_g(f)(u)(v) = \langle v, \text{Hess}(\mathcal{Q}_g)(f)(u) \rangle_X \quad \text{for } u, v \in X.$$

Next, if X is a real Hilbert space then $\text{Hess}(\mathcal{Q}_g)(f) = (\text{Hess}(\mathcal{Q}_g)(f))^*$ i.e., the Hessian $\text{Hess}(\mathcal{Q}_g)(f) \in \mathcal{L}(X, X)$ is self-adjoint. This follows from the fact that the 2nd Fréchet derivative represents a symmetric bilinear form.

We conclude with explicit expressions for the gradient $\nabla \mathcal{Q}_g(f) \in X$ and the Hessian $\text{Hess}(\mathcal{Q}_g)(f)(u) \in X$ when \mathcal{Q}_g is given as in (15):

$$\nabla \mathcal{Q}_g(f) = [\partial \mathcal{A}(f)]^* (\mathcal{A}(f) - g) \quad (66)$$

$$\begin{aligned} \text{Hess}(\mathcal{Q}_g)(f)(u) &= \left([\partial \mathcal{A}(f)]^* \circ \partial \mathcal{A}(f) \right)(u) \\ &\quad + [\partial^2 \mathcal{A}(f)(u, \cdot)]^* (\mathcal{A}(f) - g) \quad \text{for } u \in X. \end{aligned} \quad (67)$$

In particular, if $\mathcal{A}: X \rightarrow Y$ is linear, then $\partial \mathcal{A}(f) = \mathcal{A}$ independent of $f \in X$, so $\nabla \mathcal{Q}_g(f)$ is given as in (16) and $\text{Hess}(\mathcal{Q}_g)(f) = \mathcal{A}^* \circ \mathcal{A}$.

B Differentiable programming

Differentiable programming deals with techniques for differentiating computational algorithms. This relies on automatic differentiation techniques that shares traits with both symbolic and numerical differentiation. Similar to symbolic differentiation, the results are constructed out of analytic expressions and the gradients are exact (up to machine precision). Next, similar to numerical differentiation (and unlike symbolic differentiation), automatic differentiation only yields numerical values instead of symbolic expressions.

Automatic differentiation forms the core of modern deep learning frameworks since the training involves calculation of gradients. This is achieved by breaking down the computation into a series of simple computational steps, composed of elementary operations with known derivatives. While performing

the calculation, a computational graph is constructed to keep track of the values required for determining the derivatives. Such an approach does not require a full analytic expression of the model, nor even a deterministic expression. Since the necessary quantities are calculated dynamically during the evaluation of the model, branching paths, loops, and non-deterministic model architectures are automatically supported.

There are two different modes of automatic differentiation for evaluating derivatives, both with their own advantages and disadvantages. In forward mode automatic differentiation, the scalar product between the gradient and the direction is calculated in parallel with the model evaluation. This is well suited for computing derivatives when the dimension of the input space for the function being differentiated is less the dimension of the output space. In reverse mode automatic differentiation, partial derivatives are stored in memory at each node of the computational graph, enabling the calculation of the so-called adjoints in the backward pass. This approach is suitable when the dimension of the input space for the function being differentiated is larger than the dimension of the output space.

C Stochastic gradient descent (SGD)

We here provide a brief introduction to optimisation methods used for training deep neural networks. The aim is to identify some hyper parameters that are commonly varied during training. The material is based on [126, 140].

Training a deep neural network typically amounts to computing a (local) minimiser to an objective function $\mathcal{F}: \Theta \rightarrow \mathbb{R}$. This is a real-valued function defined on the set Θ of neural network parameters that one seeks to learn during training. Section 4 lists various objective functions one may encounter depending on the type of training data one has access to. As an example, the objective function for supervised data $\Sigma \subset Y \times X$ is given in (5), i.e., the objective is of the form

$$\mathcal{F}_\Sigma(\theta) := \sum_{i=1}^n \mathcal{L}_X(\mathcal{R}_\theta(g_i), f_i) \quad \text{for } \Sigma = \{(g_i, f_i)\}_{i=1}^n \subset Y \times X.$$

Objectives used in training deep neural networks are often chosen so that they are differentiable. They are however also highly non-convex and non-linear. To address the issue with non-convexity, it is common to compute a (local) minimiser by some version of SGD. The ‘stochasticity’ in SGD refers to the fact that the objective is usually not evaluated on the entire training dataset at hand, but instead on randomly sampled subsets of it (minibatches). The advantages of using minibatches are twofold: firstly, it significantly reduces the computational effort required for a parameter update. Secondly, it introduces some randomness into the minimization procedure, which can be helpful to avoid getting stuck in a local minimum. At each SGD iteration, an unbiased approximation of the gradient $\nabla_\theta \mathcal{F}_\Sigma(\theta)$ is computed. The neural network parameters are subsequently updated via:

$$\theta^{k+1} = \theta^k - \gamma_k \nabla \mathcal{F}_{\Sigma_k}(\theta).$$

Here, at each iterate one needs to choose the minibatch $\Sigma_k \subset \Sigma$ consisting of $n_k \ll n$ elements and the learning rate $\gamma_k > 0$. Numerous modifications of

this algorithm exist, which introduce additional features such as momentum or adaptive learning rates. A popular variant, which combines both of these extensions, is the Adam (adaptive moment estimation) optimizer [88], see also [20, Ch. 5] and [150, Ch. 11] for more in-depth exposition of various SGD methods and their properties.

The learning rate, choice of batch size n_k (minibatches are typically selected as random subsets of the training data), and initialisation are all hyper parameters that are typically varied during the training.

References

- [1] Wim van Aarle et al. “Fast and flexible X-ray tomography using the ASTRA toolbox”. In: *Optics Express* 24.22 (2016), pp. 25129–25147. DOI: [10.1364/OE.24.02512](https://doi.org/10.1364/OE.24.02512).
- [2] Wim van Aarle et al. “The ASTRA Toolbox: A platform for advanced algorithm development in electron tomography”. In: *Ultramicroscopy* 157 (2015), pp. 35–47. DOI: [10.1016/j.ultramic.2015.05.002](https://doi.org/10.1016/j.ultramic.2015.05.002).
- [3] Martín Abadi et al. “TensorFlow: a system for large-scale machine learning”. In: *Proceedings of the 12th USENIX conference on Operating Systems Design and Implementation Pages (OSDI’16)*. 2016, pp. 265–283.
- [4] Jonas Adler. “Learned Iterative Reconstruction”. In: *Handbook of Mathematical Models and Algorithms in Computer Vision and Imaging: Mathematical Imaging and Vision*. Ed. by Ke Chen, Carola-Bibiane Schönlieb, Xue-Cheng Tai, and Laurent Younes. Springer Verlag, 2023, pp. 751–771. DOI: [10.1007/978-3-030-98661-2_67](https://doi.org/10.1007/978-3-030-98661-2_67).
- [5] Jonas Adler and Ozan Öktem. “Learned Primal-Dual Reconstruction”. In: *IEEE Transactions on Medical Imaging* 37.6 (2018), pp. 1322–1332. DOI: [10.1109/TMI.2018.2799231](https://doi.org/10.1109/TMI.2018.2799231).
- [6] Jonas Adler and Ozan Öktem. “Solving ill-posed inverse problems using iterative deep neural networks”. In: *Inverse problems* 33.12 (2017), 124007 (24pp). DOI: [10.1088/1361-6420/aa9581](https://doi.org/10.1088/1361-6420/aa9581).
- [7] Jonas Adler, Axel Ringh, Ozan Öktem, and Johan Karlsson. *Learning to solve inverse problems using Wasserstein loss*. Published in NeurIPS Optimal Transport workshop 2017, which was part of the 31st Conference on Neural Information Processing Systems (NeurIPS 2017). 2017. DOI: [10.48550/arXiv.1710.10898](https://doi.org/10.48550/arXiv.1710.10898). arXiv: [1710.10898 \[cs.CV\]](https://arxiv.org/abs/1710.10898).
- [8] Ali Afkari-Fahandari, Elham Shabaniinia, Fatemeh Asadi-Zeydabadi, and Hossein Nezamabadi-Pour. “A Comprehensive Survey of Transformers in Text Recognition: Techniques, Challenges, and Future Directions”. In: *ACM Computing Surveys* (2025). Accepted for publication. DOI: [10.1145/3771273](https://doi.org/10.1145/3771273).
- [9] Amir Aghabiglou, Chung San Chu, Arwa Dabbech, and Yves Wiaux. “The R2D2 deep neural network series paradigm for fast precision imaging in radio astronomy”. In: *The Astrophysical Journal Supplement Series* 273.1 (2024), p. 3. DOI: [10.3847/1538-4365/ad46f5](https://doi.org/10.3847/1538-4365/ad46f5).

[10] Giovanni S. Alberti, Damiana Lazzaro, Serena Morigi, Luca Ratti, and Matteo Santacesaria. *Deep Unfolding Network for Nonlinear Multi-Frequency Electrical Impedance Tomography*. 2025. DOI: [10.48550/arXiv.2507.16678](https://doi.org/10.48550/arXiv.2507.16678) [math.NA].

[11] Martin S. Alnæs et al. “The FEniCS Project Version 1.5”. In: *Archive of Numerical Software* 3.100 (2015), pp. 9–23. DOI: [10.11588/ans.2015.100.20553](https://doi.org/10.11588/ans.2015.100.20553).

[12] Héctor Andrade-Loarca, Gitta Kutyniok, Ozan Öktem, and Philipp Petersen. “Deep microlocal reconstruction for limited-angle tomography”. In: *Applied and Computational Harmonic Analysis* 59 (2022), pp. 155–197. DOI: [10.1016/j.acha.2021.12.007](https://doi.org/10.1016/j.acha.2021.12.007).

[13] Vegard Antun, Francesco Renna, Clarice Poon, Ben Adcock, and Anders C. Hansen. “On instabilities of deep learning in image reconstruction and the potential costs of AI”. In: *Proceedings of the National Academy of Sciences of the United States of America* 117 (2020), pp. 30088–30095. DOI: [10.1073/pnas.1907377117](https://doi.org/10.1073/pnas.1907377117).

[14] Simon Arridge. “Optical tomography in medical imaging”. In: *Inverse problems* 15.2 (1999), R41. DOI: [10.1088/0266-5611/15/2/022](https://doi.org/10.1088/0266-5611/15/2/022).

[15] Simon Arridge and Andreas Hauptmann. “Networks for nonlinear diffusion problems in imaging”. In: *Journal of mathematical imaging and vision* 62.3 (2020), pp. 471–487. DOI: [10.1007/s10851-019-00901-3](https://doi.org/10.1007/s10851-019-00901-3).

[16] Simon Arridge, Andreas Hauptmann, and Yury Korolev. “Inverse problems with learned forward operators”. In: *Data-driven Models in Inverse Problems*. Ed. by Tatiana A. Bubba. Vol. 31. Radon Series on Computational and Applied Mathematics. Walter de Gruyter, 2025, pp. 73–106. DOI: <https://doi.org/10.1515/9783111251233-003>.

[17] Simon Arridge, Peter Maass, Ozan Öktem, and Carola-Bibiane Schönlieb. “Solving inverse problems using data-driven models”. In: *Acta Numerica* 28 (2019), pp. 1–174. DOI: [10.1017/S0962492919000059](https://doi.org/10.1017/S0962492919000059).

[18] Kenneth J. Arrow and Leonid Hurwicz. “Gradient method for concave programming, I: local results”. In: *Studies in Linear and Non-linear Programming*. Stanford Mathematical Studies in the Social Sciences 11. Standford, CA: Stanford University Press, 1958.

[19] Muhammad Asim, Max Daniels, Oscar Leong, Ali Ahmed, and Paul Hand. “Invertible generative models for inverse problems: mitigating representation error and dataset bias”. In: *Proceedings of Machine Learning Research: The 37th International Conference on Machine Learning (ICML 2020)*. Vol. 119. 2020, pp. 399–409.

[20] Francis Bach. *Learning Theory from First Principles*. Adaptive Computation and Machine Learning series. MIT Press, 2024.

[21] Daniel Otero Baguer, Johannes Leuschner, and Maximilian Schmidt. “Computed tomography reconstruction using deep image prior and learned reconstruction methods”. In: *Inverse Problems* 36.9 (2020), p. 094004. DOI: [10.1088/1361-6420/aba415](https://doi.org/10.1088/1361-6420/aba415).

[22] Dzmitry Bahdanau, Kyunghyun Cho, and Yoshua Bengio. *Neural Machine Translation by Jointly Learning to Align and Translate*. 2014. DOI: [10.48550/arXiv.1409.0473](https://doi.org/10.48550/arXiv.1409.0473). arXiv: [1409.0473](https://arxiv.org/abs/1409.0473) [cs.CL].

[23] Shaojie Bai, J Zico Kolter, and Vladlen Koltun. “Deep equilibrium models”. In: *Proceedings of the 33rd International Conference on Neural Information Processing Systems (NIPS’19)*. Vol. 32. 2019, 690–701 (Article no.: 63).

[24] Anatolii Borisovich Bakushinskii. “The problem of the convergence of the iteratively regularized Gauss–Newton method”. In: *Computational Mathematics and Mathematical Physics* 32.9 (1992), pp. 1353–1359.

[25] Anasua Banerjee and Debajyoti Banik. “A Comprehensive Survey on Transformer-Based Machine Translation: Identifying Research Gaps and Solutions for Large Language Models”. In: *ACM Computing Surveys* (2025). Accepted for publication. DOI: [10.1145/3773076](https://doi.org/10.1145/3773076).

[26] Sebastian Banert, Axel Ringh, Jonas Adler, Johan Karlsson, and Ozan Öktem. “Data-driven nonsmooth optimization”. In: *SIAM Journal on Optimization* 30.1 (2020), pp. 102–131. DOI: [10.1137/18M1207685](https://doi.org/10.1137/18M1207685).

[27] Sebastian Banert, Jevgenija Rudzusika, Ozan Öktem, and Jonas Adler. “Accelerated Forward–Backward Optimization using Deep Learning”. In: *SIAM Journal on Optimization* 34.2 (2024), pp. 1236–1263. DOI: [10.1137/22M1532548](https://doi.org/10.1137/22M1532548).

[28] Riccardo Barbano et al. “An educated warm start for deep image prior-based micro CT reconstruction”. In: *IEEE Transactions on Computational Imaging* 8 (2022), pp. 1210–1222. DOI: [10.1109/TCI.2022.3233188](https://doi.org/10.1109/TCI.2022.3233188).

[29] Atılım Güneş Baydin, Barak A Pearlmutter, Alexey Andreyevich Radul, and Jeffrey Mark Siskind. “Automatic differentiation in machine learning: a survey”. In: *Journal of Machine Learning Research* 18.1 (2018), pp. 5595–5637.

[30] Shabab Bazrafkan, Vincent Van Nieuwenhove, Joris Soons, Jan De Beenhouwer, and Jan Sijbers. *Deep Learning Based Computed Tomography Whys and Wherefores*. 2019. DOI: [10.48550/arXiv.1904.03908](https://doi.org/10.48550/arXiv.1904.03908). arXiv: [1904.03908 \[eess.IV\]](https://arxiv.org/abs/1904.03908).

[31] Paul Beard. “Biomedical photoacoustic imaging”. In: *Interface Focus* 1.4 (2011), pp. 602–631. DOI: [10.1098/rsfs.2011.0028](https://doi.org/10.1098/rsfs.2011.0028).

[32] Mathieu Blondel and Vincent Roulet. *The Elements of Differentiable Programming*. 2024. DOI: [10.48550/arXiv.2403.14606](https://doi.org/10.48550/arXiv.2403.14606). arXiv: [2403.14606 \[cs.LG\]](https://arxiv.org/abs/2403.14606).

[33] Ashish Bora, Ajil Jalal, Eric Price, and Alexandros G. Dimakis. “Compressed sensing using generative models”. In: *Proceedings of Machine Learning Research: The 34th International Conference on Machine Learning (ICML 2017)*. Vol. 70. 2017, pp. 537–546.

[34] Ikhlass Boukrouh, Faouzi Tayalati, and Abdellah Azmani. “Optimizing Models Performance: A Comprehensive Review and Case Study of Hyperparameters Tuning”. In: *Proceedings of Data Analytics and Management (ICDAM 2024)*. Ed. by Abhishek Swaroop, Bal Virdee, Sérgio Duarte Correia, and Zdzislaw Polkowski. Vol. 1302. Lecture Notes in Networks and Systems. 2025, pp. 69–81. DOI: [10.1007/978-981-96-3381-4_7](https://doi.org/10.1007/978-981-96-3381-4_7).

[35] Nicolas Boullé and Alex Townsend. “A mathematical guide to operator learning”. In: *Handbook of Numerical Analysis: Numerical Analysis Meets Machine Learning*. Ed. by Siddhartha Mishra and Alex Townsend. Vol. 25. Elsevier, 2024. Chap. 3, pp. 83–125. DOI: [10.1016/bs.hna.2024.05.003](https://doi.org/10.1016/bs.hna.2024.05.003).

[36] Sumanth Kumar Boya and Deepak N. Subramani. “PINTO: Physics-informed transformer neural operator for learning generalized solutions of partial differential equations for any initial and boundary condition”. In: *Computer Physics Communications* 315 (2025), p. 109702. DOI: [10.1016/j.cpc.2025.109702](https://doi.org/10.1016/j.cpc.2025.109702).

[37] James Bradbury et al. *JAX: composable transformations of Python+NumPy programs*. Version 0.2.5. 2018.

[38] Shuhao Cao. “Choose a transformer: Fourier or Galerkin”. In: *35th Conference on Neural Information Processing Systems (NeurIPS 2021)*. 2021, 24924–24940 (Article No.: 1909).

[39] Marcello Carioni, Subhadip Mukherjee, Hong Ye Tan, and Junqi Tang. “Unsupervised approaches based on optimal transport and convex analysis for inverse problems in imaging”. In: *Data-driven Models in Inverse Problems*. Ed. by Tatiana A. Bubba. Vol. 31. Radon Series on Computational and Applied Mathematics. De Gruyter, 2025, pp. 107–162. DOI: [10.1515/978311251233-004](https://doi.org/10.1515/978311251233-004).

[40] Antonin Chambolle and Thomas Pock. “A First-Order Primal-Dual Algorithm for Convex Problems with Applications to Imaging”. In: *Journal of Mathematical Imaging and Vision* 40 (2011), pp. 120–145. DOI: [10.1007/s10851-010-0251-1](https://doi.org/10.1007/s10851-010-0251-1).

[41] Stanley H. Chan, Xiran Wang, and Omar A. Elgendy. “Plug-and-play ADMM for image restoration: Fixed-point convergence and applications”. In: *IEEE Transactions on Computational Imaging* 3.1 (2016), pp. 84–98. DOI: [10.1109/TCI.2016.2629286](https://doi.org/10.1109/TCI.2016.2629286).

[42] Tianping Chen and Hong Chen. “Universal approximation to nonlinear operators by neural networks with arbitrary activation functions and its application to dynamical systems”. In: *IEEE Transactions on Neural Networks* 6.4 (1995), pp. 911–917. DOI: [10.1109/72.392253](https://doi.org/10.1109/72.392253).

[43] Yunjin Chen, Rene Ranftl, and Thomas Pock. “Insights into analysis operator learning: From patch-based sparse models to higher order MRFs”. In: *IEEE Transactions on Image Processing* 23.3 (2014), pp. 1060–1072. DOI: [10.1109/TIP.2014.2299065](https://doi.org/10.1109/TIP.2014.2299065).

[44] Yunmei Chen, Xiaojing Ye, and Qingchao Zhang. “Variational Model-Based Deep Neural Networks for Image Reconstruction”. In: *Handbook of Mathematical Models and Algorithms in Computer Vision and Imaging: Mathematical Imaging and Vision*. Ed. by Ke Chen, Carola-Bibiane Schönlieb, Xue-Cheng Tai, and Laurent Younes. Springer Verlag, 2023, pp. 879–907. DOI: [10.1007/978-3-030-98661-2_57](https://doi.org/10.1007/978-3-030-98661-2_57).

[45] Chun-Wun Cheng et al. *Continuous U-Net: Faster, Greater and Noiseless*. 2023. DOI: [10.48550/arXiv.2302.00626](https://doi.org/10.48550/arXiv.2302.00626). arXiv: [2302.00626 \[cs.CV\]](https://arxiv.org/abs/2302.00626).

[46] Vladimir Cherkassky and Eng Hock Lee. “To understand double descent, we need to understand VC theory”. In: *Neural Networks* 169 (2024), pp. 242–256. DOI: [10.1016/j.neunet.2023.10.014](https://doi.org/10.1016/j.neunet.2023.10.014).

[47] Francesco Colibazzi, Damiana Lazzaro, Serena Morigi, and Andrea Samoré. “Learning Nonlinear Electrical Impedance Tomography”. In: *Journal of Scientific Computing* 90 (2022), Article No.: 58. DOI: [10.1007/s10915-021-01716-4](https://doi.org/10.1007/s10915-021-01716-4).

[48] Giannis Daras, Joseph Dean, Ajil Jalal, and Alexandros G. Dimakis. “Intermediate layer optimization for inverse problems using deep generative models”. In: *Proceedings of Machine Learning Research: The 38th International Conference on Machine Learning (ICML 2021)*. Vol. 139. 2021, pp. 2421–2432.

[49] Leo Davy, Luis M. Briceño-Arias, and Nelly Pustelnik. “Restarted contractive operators to learn at equilibrium”. In: *Machine Learning Solutions for Inverse Problems: Part A*. Ed. by Andreas Hauptmann, Bangti Jin, and Carola-Bibiane Schönlieb. Vol. 26. Handbook of Numerical Analysis. Elsevier, 2025, pp. 315–340. DOI: <https://doi.org/10.1016/bs.hna.2025.09.006>.

[50] Sören Dittmer, Tobias Kluth, Peter Maass, and Daniel Otero Baguer. “Regularization by architecture: A deep prior approach for inverse problems”. In: *Journal of Mathematical Imaging and Vision* 62.3 (2020), pp. 456–470. DOI: [10.1007/s10851-019-00923-x](https://doi.org/10.1007/s10851-019-00923-x).

[51] Andrea Ebner and Markus Haltmeier. “Plug-and-play image reconstruction is a convergent regularization method”. In: *IEEE Transactions on Image Processing* 33 (2024), pp. 1476–1486. DOI: [10.1109/TIP.2024.3361218](https://doi.org/10.1109/TIP.2024.3361218).

[52] Jesper E. van Engelen and Holger H. Hoos. “A survey on semi-supervised learning”. In: *Machine Learning* 109 (2020), pp. 373–440. DOI: [10.1007/s10994-019-05855-6](https://doi.org/10.1007/s10994-019-05855-6).

[53] Yuwei Fan, Cindy Orozco Bohorquez, and Lexing Ying. “BCR-Net: A neural network based on the nonstandard wavelet form”. In: *Journal of Computational Physics* 384 (2019), pp. 1–15. DOI: [10.1016/j.jcp.2019.02.002](https://doi.org/10.1016/j.jcp.2019.02.002).

[54] Yuwei Fan, Jordi Feliu-Fabà, Lin Lin, Lexing Ying, and Leonardo Zepeda-Núñez. “A multiscale neural network based on hierarchical nested bases”. In: *Research in the Mathematical Sciences* 6.21 (2019), 28 pp. DOI: [10.1007/s40687-019-0183-3](https://doi.org/10.1007/s40687-019-0183-3).

[55] Yuwei Fan, Lin Lin, Lexing Ying, and Leonardo Zepeda-Núñez. “A Multiscale Neural Network Based on Hierarchical Matrices”. In: *Multiscale Modeling & Simulation* 17.4 (2019), pp. 1–15. DOI: [10.1137/18M1203602](https://doi.org/10.1137/18M1203602).

[56] Jordi Feliu-Fabà, Yuwei Fan, and Lexing Ying. “Meta-learning pseudo-differential operators with deep neural networks”. In: *Journal of Computational Physics* 408 (2020), 109309 (18 pp.) DOI: [10.1016/j.jcp.2020.109309](https://doi.org/10.1016/j.jcp.2020.109309).

[57] Lin Fu and Bruno De Man. “Deep learning tomographic reconstruction through hierarchical decomposition of domain transforms”. In: *Visual Computing for Industry, Biomedicine, and Art* 5 (2022), Article No.: 30. DOI: [10.1186/s42492-022-00127-y](https://doi.org/10.1186/s42492-022-00127-y).

[58] Samy Wu Fung et al. “Jfb: Jacobian-free backpropagation for implicit networks”. In: *Proceedings of the AAAI Conference on Artificial Intelligence*. Vol. 36. 6. 2022, pp. 6648–6656.

[59] Davis Gilton, Gregory Ongie, and Rebecca Willett. “Deep equilibrium architectures for inverse problems in imaging”. In: *IEEE Transactions on Computational Imaging* 7 (2021), pp. 1123–1133. DOI: [10.1109/TCI.2021.3118944](https://doi.org/10.1109/TCI.2021.3118944).

[60] Gerardo González, Ville Kolehmainen, and Aku Seppänen. “Isotropic and anisotropic total variation regularization in electrical impedance tomography”. In: *Computers & Mathematics with Applications* 74.3 (2017), pp. 564–576.

[61] Karol Gregor and Yann LeCun. “Learning fast approximations of sparse coding”. In: *Proceedings of the 27th International Conference on International Conference on Machine Learning (ICML’10)*. 2010, pp. 399–406.

[62] Janek Gröhl et al. “Digital twins enable full-reference quality assessment of photoacoustic image reconstructions”. In: *The Journal of the Acoustical Society of America* 158.1 (July 2025), pp. 590–601. DOI: [10.1121/10.0037188](https://doi.org/10.1121/10.0037188).

[63] Steven Guan, Ko-Tsung Hsu, and Parag V. Chitnis. “Fourier Neural Operator Network for Fast Photoacoustic Wave Simulations”. In: *Algorithms* 16.2 (2023). DOI: [10.3390/a16020124](https://doi.org/10.3390/a16020124).

[64] Luying Gui, Jun Ma, and Xiaoping Yang. “Variational Models and Their Combinations with Deep Learning in Medical Image Segmentation: A Survey”. In: *Handbook of Mathematical Models and Algorithms in Computer Vision and Imaging: Mathematical Imaging and Vision*. Ed. by Ke Chen, Carola-Bibiane Schönlieb, Xue-Cheng Tai, and Laurent Younes. Springer Verlag, 2023, pp. 1001–1022. DOI: [10.1007/978-3-030-98661-2_109](https://doi.org/10.1007/978-3-030-98661-2_109).

[65] Eldad Haber and Lars Ruthotto. “Stable architectures for deep neural networks”. In: *Inverse problems* 34.1 (2017), p. 014004. DOI: [10.1088/1361-6420/aa9a90](https://doi.org/10.1088/1361-6420/aa9a90).

[66] Kerstin Hammernik et al. “Learning a variational network for reconstruction of accelerated MRI data”. In: *Magnetic resonance in medicine* 79.6 (2018), pp. 3055–3071. DOI: [10.1002/mrm.26977](https://doi.org/10.1002/mrm.26977).

[67] Zhongkai Hao et al. “GNOT: A General Neural Operator Transformer for Operator Learning”. In: *Journal of Machine Learning Research* 202 (2023). Proceedings of the 40th International Conference on Machine (ICML 2023), 12556–12569 (Article No.: 509).

[68] Andreas Hauptmann, Jonas Adler, Simon Arridge, and Ozan Öktem. “Multi-scale learned iterative reconstruction”. In: *IEEE transactions on computational imaging* 6 (2020), pp. 843–856. DOI: [10.1109/TCI.2020.2990299](https://doi.org/10.1109/TCI.2020.2990299).

[69] Andreas Hauptmann, Leonid Kunyansky, and Jenni Poimala. *Fast algorithms enabling optimization and deep learning for photoacoustic tomography in a circular detection geometry*. 2025. DOI: [10.48550/arXiv.2510.24687](https://doi.org/10.48550/arXiv.2510.24687). arXiv: [2510.24687 \[eess.IV\]](https://arxiv.org/abs/2510.24687).

[70] Andreas Hauptmann, Subhadip Mukherjee, Carola-Bibiane Schönlieb, and Ferdia Sherry. “Convergent regularization in inverse problems and linear plug-and-play denoisers”. In: *Foundations of Computational Mathematics* (2024), pp. 1–34. DOI: [10.1007/s10208-024-09654-x](https://doi.org/10.1007/s10208-024-09654-x).

[71] Andreas Hauptmann and Jenni Poimala. *Model-corrected learned primal-dual models for fast limited-view photoacoustic tomography*. 2023. DOI: [10.48550/arXiv.2304.01963](https://doi.org/10.48550/arXiv.2304.01963). arXiv: [2304.01963 \[eess.IV\]](https://arxiv.org/abs/2304.01963 [eess.IV]).

[72] Andreas Hauptmann et al. “Approximate k-space models and deep learning for fast photoacoustic reconstruction”. In: *Machine Learning for Medical Image Reconstruction (MLMIR 2018), held in Conjunction with MICCAI 2018*. Ed. by Florian Knoll, Andreas Maier, and Daniel Rueckert. Lecture Notes in Computer Science 11074. Springer Verlag, 2018, pp. 103–111. DOI: [10.1007/978-3-030-00129-2_12](https://doi.org/10.1007/978-3-030-00129-2_12).

[73] Andreas Hauptmann et al. “Model-Based Learning for Accelerated, Limited-View 3-D Photoacoustic Tomography”. In: *IEEE Transactions on Medical Imaging* 37.6 (2018), pp. 1382–1393. DOI: [10.1109/TMI.2018.2820382](https://doi.org/10.1109/TMI.2018.2820382).

[74] Kaiming He, Xiangyu Zhang, Shaoqing Ren, and Jian Sun. “Deep Residual Learning for Image Recognition”. In: *IEEE Conference on Computer Vision and Pattern Recognition, CVPR* (2016), pp. 770–778. DOI: [10.1109/CVPR.2016.90](https://doi.org/10.1109/CVPR.2016.90).

[75] William Herzberg, Andreas Hauptmann, and Sarah J Hamilton. “Domain independent post-processing with graph U-nets: applications to electrical impedance tomographic imaging”. In: *Physiological measurement* 44.12 (2023), p. 125008. DOI: [10.1088/1361-6579/ad0b3d](https://doi.org/10.1088/1361-6579/ad0b3d).

[76] William Herzberg, Daniel B Rowe, Andreas Hauptmann, and Sarah J Hamilton. “Graph convolutional networks for model-based learning in nonlinear inverse problems”. In: *IEEE transactions on computational imaging* 7 (2021), pp. 1341–1353. DOI: [10.1109/TCI.2021.3132190](https://doi.org/10.1109/TCI.2021.3132190).

[77] Yuanming Hu et al. “DiffTaichi: Differentiable programming for physical simulation”. In: *8th International Conference on Learning Representations (ICLR 2020)*. 2020.

[78] Samuel Hurault, Ulugbek Kamilov, Arthur Leclaire, and Nicolas Papadakis. “Convergent bregman plug-and-play image restoration for poisson inverse problems”. In: *Advances in Neural Information Processing Systems* 36 (2023), pp. 27251–27280.

[79] Samuel Hurault, Arthur Leclaire, and Nicolas Papadakis. “Gradient Step Denoiser for convergent Plug-and-Play”. In: *10th International Conference on Learning Representations (ICLR 2022)*. 2022.

[80] Anastasia Ioannidou, Elisavet Chatzilari, Spiros Nikolopoulos, and Ioannis Kompatsiaris. “Deep Learning Advances in Computer Vision with 3D Data: A Survey”. In: *ACM Computing Surveys* 50.2 (2017), Article No.: 20 (38 pp.) DOI: [10.1145/3042064](https://doi.org/10.1145/3042064).

[81] Wenzel Jakob et al. *Mitsuba 3 renderer*. Version 3.1.1. <https://mitsuba-renderer.org>. 2022.

[82] Kyong Hwan Jin, Michael T. McCann, Emmanuel Froustey, and Michael Unser. “Deep Convolutional Neural Network for Inverse Problems in Imaging”. In: *IEEE Transactions on Image Processing* 26.9 (2017), pp. 4509–4522. DOI: [10.1109/TIP.2017.2713099](https://doi.org/10.1109/TIP.2017.2713099).

[83] Preetish Kakkar, Srijani Mukherjee, Hariharan Ragothaman, and Vishal Mehta. “Physics Based Differentiable Rendering for Inverse Problems and Beyond”. In: *Journal of Electrical Systems* 20.11 (2024). DOI: [10.52783/jes.7210](https://doi.org/10.52783/jes.7210).

[84] Ulugbek S Kamilov, Charles A Bouman, Gregery T Buzzard, and Brendt Wohlberg. “Plug-and-play methods for integrating physical and learned models in computational imaging: Theory, algorithms, and applications”. In: *IEEE Signal Processing Magazine* 40.1 (2023), pp. 85–97. DOI: [10.1109/MSP.2022.3199595](https://doi.org/10.1109/MSP.2022.3199595).

[85] Eunhee Kang, Junhong Min, and Jong Chul Ye. “A deep convolutional neural network using directional wavelets for low-dose X-ray CT reconstruction”. In: *Medical physics* 44.10 (2017), e360–e375. DOI: [10.1002/mp.12344](https://doi.org/10.1002/mp.12344).

[86] Tero Karras et al. “Alias-free generative adversarial networks”. In: *35th Conference on Neural Information Processing Systems (NeurIPS 2021)*. 2021, 852–863 (Article No.: 66).

[87] Salman Khan et al. “Transformers in Vision: A Survey”. In: *ACM Computing Surveys* 54.10 (2022), Article No.: 200 (41 pp.) DOI: [10.1145/3505244](https://doi.org/10.1145/3505244).

[88] Diederik P. Kingma and Jimmy Ba. “Adam: A method for stochastic optimization”. In: *6th International Conference on Learning Representations (ICLR 2015)*. 2015.

[89] Teresa Klatzer, Savvas Melidonis, Marcelo Pereyra, and Konstantinos C Zygalis. *Efficient Bayesian Computation Using Plug-and-Play Priors for Poisson Inverse Problems*. 2025. DOI: [10.48550/arXiv.2503.16222](https://doi.org/10.48550/arXiv.2503.16222). arXiv: [2503.16222 \[stat.CO\]](https://arxiv.org/abs/2503.16222).

[90] Erich Kobler, Alexander Effland, Karl Kunisch, and Thomas Pock. “Total deep variation for linear inverse problems”. In: *Proceedings of the IEEE/CVF Conference on computer vision and pattern recognition (CVPR)*. 2020, pp. 7549–7558. DOI: [10.1109/CVPR42600.2020.00757](https://doi.org/10.1109/CVPR42600.2020.00757).

[91] Erich Kobler, Alexander Effland, Karl Kunisch, and Thomas Pock. “Total Deep Variation: A Stable Regularization Method for Inverse Problems”. In: *IEEE Transactions on Pattern Analysis and Machine Intelligence* 44.12 (2022), pp. 9163–9180. DOI: [10.1109/TPAMI.2021.3124086](https://doi.org/10.1109/TPAMI.2021.3124086).

[92] Erich Kobler, Teresa Klatzer, Kerstin Hammernik, and Thomas Pock. “Variational networks: connecting variational methods and deep learning”. In: *Pattern Recognition Proceedings of the 39th German Conference (GCPR 2017), Basel, Switzerland, September 12–15, 2017*. Ed. by Volker Roth and Thomas Vetter. Vol. 10496. Lecture Notes in Computer Science. 2017, pp. 281–293. DOI: [10.1007/978-3-319-66709-6_23](https://doi.org/10.1007/978-3-319-66709-6_23).

[93] Nikola Kovachki et al. “Neural operator: Learning maps between function spaces with applications to PDEs”. In: *Journal of Machine Learning Research* 24.89 (2023), pp. 1–97.

[94] Nikola B. Kovachki, Samuel Lanthaler, and Andrew M. Stuart. “Operator learning: Algorithms and analysis”. In: *Handbook of Numerical Analysis: Numerical Analysis Meets Machine Learning*. Ed. by Siddhartha Mishra and Alex Townsend. Vol. 25. Elsevier, 2024. Chap. 9, pp. 419–467. DOI: [10.1016/bs.hna.2024.05.009](https://doi.org/10.1016/bs.hna.2024.05.009).

[95] Marc Lafon and Alexandre Thomas. *Understanding the Double Descent Phenomenon in Deep Learning*. 2024. DOI: [10.48550/arXiv.2403.10459](https://doi.org/10.48550/arXiv.2403.10459) [cs.LG]. arXiv: [2403.10459 \[cs.LG\]](https://arxiv.org/abs/2403.10459).

[96] Yann LeCun, Yoshua Bengio, and Geoffrey Hinton. “Deep learning”. In: *Nature* 521 (2015), pp. 436–444. DOI: [10.1038/nature14539](https://doi.org/10.1038/nature14539).

[97] Jiawei Li et al. “Fundamental Capabilities and Applications of Large Language Models: A Survey”. In: *ACM Computing Surveys* 58.2 (2025), Article No.: 38 (42 pp.) DOI: [10.1145/3735632](https://doi.org/10.1145/3735632).

[98] Yingzhou Li, Xiuyuan Cheng, and Jianfeng Lu. *Butterfly-Net: Optimal Function Representation Based on Convolutional Neural Networks*. 2018. DOI: [10.48550/arXiv.1805.07451](https://doi.org/10.48550/arXiv.1805.07451). arXiv: [1805.07451 \[math.NA\]](https://arxiv.org/abs/1805.07451).

[99] Zongyi Li et al. “Fourier Neural Operator for Parametric Partial Differential Equations”. In: *International Conference on Learning Representations (ICLR 2021)*. 2021.

[100] Min Lin. “Automatic Functional Differentiation in JAX”. In: *International Conference on Representation Learning 2024 (ICLR 2024)*. 2024.

[101] Wei-An Lin et al. “DuDoNet: Dual domain network for CT metal artifact reduction”. In: *Proceedings of the IEEE/CVF Conference on Computer Vision and Pattern Recognition (CVPR)*. 2019, pp. 10512–10521. DOI: [10.1109/CVPR.2019.01076](https://doi.org/10.1109/CVPR.2019.01076).

[102] Shengjun Liu et al. “Architectures, variants, and performance of neural operators: A comparative review”. In: *Neurocomputing* 648 (2025), p. 130518. DOI: [10.1016/j.neucom.2025.130518](https://doi.org/10.1016/j.neucom.2025.130518).

[103] Anders Logg, Kent-Andre Mardal, and Garth Wells. *Automated Solution of Differential Equations by the Finite Element Method: The FEniCS Book*. Vol. 84. Lecture Notes in Computational Science and Engineering. Springer Verlag, 2012. DOI: [10.1007/978-3-642-23099-8](https://doi.org/10.1007/978-3-642-23099-8).

[104] Anders Logg and Garth N. Wells. “DOLFIN: Automated finite element computing”. In: *ACM Transactions on Mathematical Software* 37.2 (2010), Article No.: 20 (28 pp.) DOI: [10.1145/1731022.1731030](https://doi.org/10.1145/1731022.1731030).

[105] Sebastian Lunz. “Learned Regularizers for Inverse Problems”. In: *Handbook of Mathematical Models and Algorithms in Computer Vision and Imaging: Mathematical Imaging and Vision*. Ed. by Ke Chen, Carola-Bibiane Schönlieb, Xue-Cheng Tai, and Laurent Younes. Springer Verlag, 2023, pp. 1133–1153. DOI: [10.1007/978-3-030-98661-2_68](https://doi.org/10.1007/978-3-030-98661-2_68).

[106] Sebastian Lunz, Andreas Hauptmann, Tanja Tarvainen, Carola-Bibiane Schönlieb, and Simon Arridge. “On learned operator correction in inverse problems”. In: *SIAM Journal on Imaging Sciences* 14.1 (2021), pp. 92–127. DOI: [10.1137/20M1338460](https://doi.org/10.1137/20M1338460).

[107] Junyu Luo et al. *Semi-supervised Fine-tuning for Large Language Models*. 2024. DOI: [10.48550/arXiv.2410.14745](https://doi.org/10.48550/arXiv.2410.14745). arXiv: [2410.14745 \[cs.CL\]](https://arxiv.org/abs/2410.14745).

[108] Anssi Manninen, Janek Gröhl, Felix Lucka, and Andreas Hauptmann. *Towards robust quantitative photoacoustic tomography via learned iterative methods*. 2025. DOI: [10.48550/arXiv.2510.27487](https://doi.org/10.48550/arXiv.2510.27487). arXiv: [2510.27487 \[eess.IV\]](https://arxiv.org/abs/2510.27487).

[109] Youngjae Min and Navid Azizan. *HardNet: Hard-Constrained Neural Networks with Universal Approximation Guarantees*. 2025. DOI: [10.48550/arXiv.2410.10807](https://doi.org/10.48550/arXiv.2410.10807). arXiv: [2410.10807 \[cs.LG\]](https://arxiv.org/abs/2410.10807).

[110] Vishal Monga, Yuelong Li, and Yonina C. Eldar. “Algorithm Unrolling: Interpretable, efficient deep learning for signal and image processing”. In: *IEEE Signal Processing Magazine* 38.2 (Mar. 2021), pp. 18–44. DOI: [10.1109/MSP.2020.3016905](https://doi.org/10.1109/MSP.2020.3016905).

[111] Meghdoot Mozumder, Andreas Hauptmann, Ilkka Nissilä, Simon R. Arridge, and Tanja Tarvainen. “A Model-Based Iterative Learning Approach for Diffuse Optical Tomography”. In: *IEEE Transactions on Medical Imaging* 41.5 (2022), pp. 1289–1299. DOI: [10.1109/TMI.2021.3136461](https://doi.org/10.1109/TMI.2021.3136461).

[112] Subhadip Mukherjee, Marcello Carioni, Ozan Öktem, and Carola-Bibiane Schönlieb. “End-to-end reconstruction meets data-driven regularization for inverse problems”. In: *Advances in Neural Information Processing Systems* 34 (2021), pp. 21413–21425.

[113] Subhadip Mukherjee, Andreas Hauptmann, Ozan Öktem, Marcelo Pereyra, and Carola-Bibiane Schönlieb. “Learned Reconstruction Methods With Convergence Guarantees: A survey of concepts and applications”. In: *IEEE Signal Processing Magazine* 40.1 (2023), pp. 164–182. DOI: [10.1109/MSP.2022.3207451](https://doi.org/10.1109/MSP.2022.3207451).

[114] Pravin Nair, Ruturaj G. Gavaskar, and Kunal Narayan Chaudhury. “Fixed-point and objective convergence of plug-and-play algorithms”. In: *IEEE Transactions on Computational Imaging* 7 (2021), pp. 337–348. DOI: [10.1109/TCI.2021.3066053](https://doi.org/10.1109/TCI.2021.3066053).

[115] Nicholas H. Nelsen and Yunan Yang. *Operator learning meets inverse problems: A probabilistic perspective*. 2025. DOI: [10.48550/arXiv.2508.20207](https://doi.org/10.48550/arXiv.2508.20207). arXiv: [2508.20207 \[math.NA\]](https://arxiv.org/abs/2508.20207).

[116] Rhys Newbury et al. “A Review of Differentiable Simulators”. In: *IEEE Access* 12 (2024). DOI: [10.1109/ACCESS.2024.3425448](https://doi.org/10.1109/ACCESS.2024.3425448).

[117] Changheun Oh, Dongchan Kim, Jun-Young Chung, Yeji Han, and Hyun-Wook Park. “ETER-net: End to End MR Image Reconstruction Using Recurrent Neural Network”. In: *International Workshop on Machine Learning for Medical Image Reconstruction (MLMIR 2018)*. Ed. by Florian Knoll, Andreas Maier, and Daniel Rueckert. Vol. 11074. Lecture Notes in Computer Science. Springer Verlag, 2018, pp. 12–20. DOI: [10.1007/978-3-030-00129-2_2](https://doi.org/10.1007/978-3-030-00129-2_2).

[118] Sebastian Lunz and Ozan Öktem and Carola-Bibiane Schönlieb. “Adversarial regularizers in inverse problems”. In: *Proceedings of the 32nd International Conference on Neural Information Processing Systems (NIPS’18)*. 2018, pp. 8516–8525.

[119] Adam Paszke et al. “PyTorch: an imperative style, high-performance deep learning library”. In: *Proceedings of the 33rd International Conference on Neural Information Processing Systems (NeurIPS 2019)*. 2019, 8026–8037 (Article No.: 721).

[120] Philipp Probst, Anne-Laure Boulesteix, and Bernd Bischl. “Tunability: Importance of Hyperparameters of Machine Learning Algorithms”. In: *Journal of Machine Learning Research* 20.1 (2019), pp. 1934–1965.

[121] Patrick Putzky and Max Welling. *Recurrent Inference Machines for Solving Inverse Problems*. 2017. doi: [10.48550/arXiv.1706.04008](https://doi.org/10.48550/arXiv.1706.04008). arXiv: [1706.04008 \[cs.NE\]](https://arxiv.org/abs/1706.04008).

[122] Mohaimenul Azam Khan Raiaan et al. “A systematic review of hyperparameter optimization techniques in Convolutional Neural Networks”. In: *Decision Analytics Journal* 11 (2024), p. 100470. doi: [10.1016/j.dajour.2024.100470](https://doi.org/10.1016/j.dajour.2024.100470).

[123] Bogdan Raonić et al. “Convolutional Neural Operators for robust and accurate learning of PDEs”. In: *37th Conference on Neural Information Processing Systems (NeurIPS 2023)*. 2023, 77187–77200 (Article No.: 3376).

[124] Stefan Roth and Michael J Black. “Fields of experts”. In: *International Journal of Computer Vision* 82.2 (2009), pp. 205–229. doi: [10.1007/s11263-008-0197-6](https://doi.org/10.1007/s11263-008-0197-6).

[125] Stefan Roth and Michael J Black. “Fields of experts: A framework for learning image priors”. In: *2005 IEEE Computer Society Conference on Computer Vision and Pattern Recognition (CVPR’05)*. Vol. 2. IEEE. 2005, pp. 860–867. doi: [10.1109/CVPR.2005.160](https://doi.org/10.1109/CVPR.2005.160).

[126] Sebastian Ruder. *An overview of gradient descent optimization algorithms*. 2016. doi: [10.48550/arXiv.1609.04747](https://doi.org/10.48550/arXiv.1609.04747). arXiv: [1609.04747 \[cs.LG\]](https://arxiv.org/abs/1609.04747).

[127] Jevgenija Rudzusika, Buda Bajić, Thomas Koehler, and Ozan Öktem. “3D helical CT Reconstruction with a Memory Efficient Learned Primal-Dual Architecture”. In: *IEEE Transactions on Computational Imaging* 10 (2024), pp. 1414–1424. doi: [10.1109/TCI.2024.3463485](https://doi.org/10.1109/TCI.2024.3463485).

[128] Christina Runkel, Ander Biguri, and Carola-Bibiane Schönlieb. “Continuous Learned Primal Dual”. In: *2024 IEEE 34th International Workshop on Machine Learning for Signal Processing (MLSP)*. 2024. doi: [10.1109/MLSP58920.2024.10734760](https://doi.org/10.1109/MLSP58920.2024.10734760).

[129] Lars Ruthotto and Eldad Haber. “Deep Neural Networks Motivated by Partial Differential Equations”. In: *Journal of Mathematical Imaging and Vision* 62 (2020), pp. 352–364. doi: [10.1007/s10851-019-00903-1](https://doi.org/10.1007/s10851-019-00903-1).

[130] Ernest Ryu et al. “Plug-and-Play Methods Provably Converge with Properly Trained Denoisers”. In: *Proceedings of the 36th International Conference on Machine Learning*. Ed. by Kamalika Chaudhuri and Ruslan Salakhutdinov. Vol. 97. Proceedings of Machine Learning Research. Long Beach, California, USA: PMLR, 2019, pp. 5546–5557.

[131] Antti Sällinen. “On comparison of learned reconstructions in supervised and unsupervised training settings with Noise2Inverse”. MA thesis. University of Oulu, 2024.

[132] Rylan Schaeffer et al. *Double Descent Demystified: Identifying, Interpreting & Ablating the Sources of a Deep Learning Puzzle*. ICLR 2024 BlogPost. 2024.

[133] Christian J. Schuler, Michael Hirsch, Stefan Harmeling, and Bernhard Schölkopf. “Learning to deblur”. In: *IEEE Transactions on Pattern Analysis and Machine Intelligence* 38.7 (2016), pp. 1439–1451. DOI: [10.1109/TPAMI.2015.2481418](https://doi.org/10.1109/TPAMI.2015.2481418).

[134] Viraj Shah and Chinmay Hegde. “Solving linear inverse problems using GAN priors: An algorithm with provable guarantees”. In: *2018 IEEE International Conference on Acoustics, Speech and Signal Processing (ICASSP)*. 2018, pp. 4609–4613. DOI: [10.1109/ICASSP.2018.8462233](https://doi.org/10.1109/ICASSP.2018.8462233).

[135] Benjamin Shih, Ahmad Peyvan, Zhongqiang Zhang, and George Em Karniadakis. “Transformers as neural operators for solutions of differential equations with finite regularity”. In: *Computer Methods in Applied Mechanics and Engineering* 434 (2025), p. 117560. DOI: [10.1016/j.cma.2024.117560](https://doi.org/10.1016/j.cma.2024.117560).

[136] Danny Smyl, Tyler N Tallman, Dong Liu, and Andreas Hauptmann. “An efficient quasi-Newton method for nonlinear inverse problems via learned singular values”. In: *IEEE Signal Processing Letters* 28 (2021), pp. 748–752. DOI: [10.1109/LSP.2021.3063622](https://doi.org/10.1109/LSP.2021.3063622).

[137] Emanuel Ström, Mats Persson, Alma Eguizabal, and Ozan Öktem. “Photon-counting CT reconstruction with a learned forward operator”. In: *IEEE Transactions on Computational Imaging* 8 (2022), pp. 536–550. DOI: [10.1109/TCI.2022.3183405](https://doi.org/10.1109/TCI.2022.3183405).

[138] Julián Tachella et al. *DeepInverse: A Python package for solving imaging inverse problems with deep learning*. 2025. DOI: [10.48550/arXiv.2505.20160](https://doi.org/10.48550/arXiv.2505.20160). arXiv: [2505.20160 \[eess.IV\]](https://arxiv.org/abs/2505.20160).

[139] Xue-Cheng Tai, Hao Liu, Raymond H. Chan, and Lingfeng Li. “A mathematical explanation of UNet”. In: *Mathematical Foundations of Computing* 8.5 (2025), pp. 874–889. DOI: [10.3934/mfc.2024040](https://doi.org/10.3934/mfc.2024040).

[140] Yingjie Tian, Yuqi Zhang, and Haibin Zhang. “Recent Advances in Stochastic Gradient Descent in Deep Learning”. In: *Mathematics* 11.3 (2023), p. 682. DOI: [10.3390/math11030682](https://doi.org/10.3390/math11030682).

[141] J. Toivanen et al. “Graph convolutional networks enable fast hemorrhagic stroke monitoring with electrical impedance tomography”. In: *IEEE Transactions on Biomedical Engineering* (2025), pp. 1–11. DOI: [10.1109/TBME.2025.3594249](https://doi.org/10.1109/TBME.2025.3594249).

[142] Singanallur V. Venkatakrishnan, Charles A. Bouman, and Brendt Wohlberg. “Plug-and-play priors for model based reconstruction”. In: *2013 IEEE Global Conference on Signal and Information Processing*. IEEE. 2013, pp. 945–948. DOI: [10.1109/GlobalSIP.2013.6737048](https://doi.org/10.1109/GlobalSIP.2013.6737048).

[143] Radoslav G. Vuchkov, Cosmin G. Petra, and Noémi Petra. “On the Derivation of Quasi-Newton Formulas for Optimization in Function Spaces”. In: *Numerical Functional Analysis and Optimization* 41.13 (2020), pp. 1564–1587. DOI: [10.1080/01630563.2020.1785496](https://doi.org/10.1080/01630563.2020.1785496).

[144] Luping Wang et al. “Parameter-efficient fine-tuning in large language models: a survey of methodologies”. In: *Artificial Intelligence Review* 58 (2025), Article No.: 227 (64 pp.) DOI: [10.1007/s10462-025-11236-4](https://doi.org/10.1007/s10462-025-11236-4).

[145] Zhengwei Wang, Qi She, and Tomás E. Ward. “Generative Adversarial Networks in Computer Vision: A Survey and Taxonomy”. In: *ACM Computing Surveys* 54.2 (2021), Article No.: 37 (38 pp.) DOI: [10.1145/3439723](https://doi.org/10.1145/3439723).

[146] Hilde J. P. Weerts, Andreas C. Mueller, and Joaquin Vanschoren. *Importance of Tuning Hyperparameters of Machine Learning Algorithms*. 2022. DOI: [10.48550/arXiv.2007.07588](https://doi.org/10.48550/arXiv.2007.07588). arXiv: [2007.07588 \[cs.LG\]](https://arxiv.org/abs/2007.07588).

[147] Weihao Xia et al. “GAN Inversion: A Survey”. In: *IEEE Transactions on Pattern Analysis and Machine Intelligence* 45.3 (2023), pp. 3121–3138. DOI: [10.1109/TPAMI.2022.3181070](https://doi.org/10.1109/TPAMI.2022.3181070).

[148] Li Yang and Abdallah Shami. “On hyperparameter optimization of machine learning algorithms: Theory and practice”. In: *Neurocomputing* 415 (2020), pp. 295–316. DOI: [10.1016/j.neucom.2020.07.061](https://doi.org/10.1016/j.neucom.2020.07.061).

[149] Shukang Yin et al. “A survey on multimodal large language models”. In: *National Science Review* 11.12 (2024). DOI: [10.1093/nsr/nwae403](https://doi.org/10.1093/nsr/nwae403).

[150] Aston Zhang, Zack C. Lipton, Mu Li, and Alex J. Smola. *Dive into Deep Learning*. Online book. 2025.

[151] Haopeng Zhang, Philip S. Yu, and Jiawei Zhang. “A Systematic Survey of Text Summarization: From Statistical Methods to Large Language Models”. In: *ACM Computing Surveys* 57.11 (2025), Article No.: 277 (41 pp.) DOI: [10.1145/3731445](https://doi.org/10.1145/3731445).

[152] Keyao Zhang et al. *GoCkpt: Gradient-Assisted Multi-Step overlapped Checkpointing for Efficient LLM Training*. 2025. DOI: [10.48550/arXiv.2511.07035](https://doi.org/10.48550/arXiv.2511.07035). arXiv: [2511.07035 \[cs.OS\]](https://arxiv.org/abs/2511.07035).

[153] Shuang Zhao, Wenzel Jakob, and Tzu-Mao Li. “Physics-based differentiable rendering: from theory to implementation”. In: *ACM SIGGRAPH 2020 Courses*. 2020, Article No.: 14 (30 pp.) DOI: [10.1145/3388769.3407454](https://doi.org/10.1145/3388769.3407454).

[154] Bo Zhu, Jeremiah Z. Liu, Stephen F. Cauley, Bruce R. Rosen, and Matthew S. Rosen. “Image reconstruction by domain-transform manifold learning”. In: *Nature* 555 (2018), pp. 487–492. DOI: [10.1038/nature25988](https://doi.org/10.1038/nature25988).

[155] Aya M. Al-Zoghby, Esraa Mohamed K. Al-Awadly, Ahmed Ismail Ebada, and Wael A. Awad. “Overview of Multimodal Machine Learning”. In: *ACM Transactions on Asian and Low-Resource Language Information Processing* 24.1 (2025), Article No.: 10 (20 pp.) DOI: [10.1145/3701031](https://doi.org/10.1145/3701031).